NASA TR R-122

NASA TR R-122

LOAN COPY:
AFSWC
KIRTLAND

TECH LIBRARY KAFB, NM
0068201

NATIONAL AERONAUTICS AND SPACE ADMINISTRATION

TECHNICAL REPORT
R-122

PARAMETER STUDY OF INSERTION CONDITIONS FOR LUNAR MISSIONS INCLUDING VARIOUS TRAJECTORY CONSIDERATIONS

By CARL R. HUSS, HAROLD A. HAMER,
and JOHN P. MAYER

1961

For sale by the Superintendent of Documents, U.S. Government Printing Office, Washington, D.C., 20402. Yearly subscription, $15: foreign, $19; single copy price varies according to size - - - - - - - - - Price 50 cents

TECH LIBRARY KAFB, NM

0068201

TECHNICAL REPORT R-122

PARAMETER STUDY OF INSERTION CONDITIONS FOR LUNAR MISSIONS INCLUDING VARIOUS TRAJECTORY CONSIDERATIONS

By CARL R. HUSS, HAROLD A. HAMER, and JOHN P. MAYER

Langley Research Center
Langley Air Force Base, Va.

CONTENTS

	Page
SUMMARY	1
INTRODUCTION	1
ASSUMPTIONS AND METHOD	2
RANGE OF PARAMETERS	2
RESULTS AND DISCUSSION	3
Lunar Approach Trajectories	3
Impact boundaries	3
Minimum insertion velocity for impact	6
Dead-center hits	7
Specified lunar miss distances	7
Velocity at closest approach to moon	9
Longitude limits of lunar impact	16
Longitude of closest approach to moon	17
Trip times to closest approach to moon	17
Earth Return Trajectories	18
Return to earth within a specified perigee	18
Total trip times for return to earth	23
Effects of Assumed Lunar Orbit	24
Errors caused by assumed lunar orbit	25
Insertion-condition corrections for true lunar orbit	25
VALIDATION OF RESULTS	26
CONCLUDING REMARKS	30
APPENDIX A—SYMBOLS	31
APPENDIX B—EQUATIONS OF MOTION	33
APPENDIX C—SPHERES OF INFLUENCE OF MOON AND EARTH	42
Sphere of Influence of Moon	42
Sphere of Influence of Earth	43
REFERENCES	43

TECHNICAL REPORT R-122

PARAMETER STUDY OF INSERTION CONDITIONS FOR LUNAR MISSIONS INCLUDING VARIOUS TRAJECTORY CONSIDERATIONS

By CARL R. HUSS, HAROLD A. HAMER, and JOHN P. MAYER

SUMMARY

A parameter study of lunar ballistic trajectories was made with the use of the restricted two-body orbit equations. A sphere of influence was assumed to exist about the earth and about the moon so that the attraction of each body on the vehicle could be treated separately. The earth and moon were considered as point masses, and the lunar orbit was assumed to be circular. The motion of the vehicle was confined to the plane defined by the lunar orbit.

The results of the study are summarized as charts from which approximate insertion conditions (velocity, radius vector or altitude, flight-path angle, and lunar lead angle or firing time) can be selected for specific lunar miss distances. The charts also provide insertion requirements for returning within a specified distance from the earth and information on vehicle velocity at perilune (closest approach to moon), longitude of perilune, longitude of impact, trip time to the moon, and total trip time for return to earth. The results of this study serve as good first approximations for the initial inputs to the more sophisticated equations of motion ordinarily used in lunar trajectory analysis.

The range of insertion altitudes studied was from 90 to 1,040 statute miles, and the range of insertion flight-path angles was from 0° to 60°. The insertion velocities varied from the minimum value required to enter the lunar sphere of influence up to a value of 80,000 ft/sec. The range of lunar lead angles covered all possible values resulting in ballistic trajectories that entered the lunar sphere of influence. In most of the calculations the moon was assumed to be at its average distance from the earth; some data are included with the moon at the two extremes in its actual orbit.

INTRODUCTION

The advent of the lunar mission and the ready access to automatic computing equipment have led to various studies of lunar trajectories. In order to calculate the trajectory for a particular mission, the initial inputs (insertion conditions) which satisfy the mission requirements must be known. Information of this type is limited because the majority of trajectory calculations have been made for a specific mission and/or a specific vehicle performance. Consequently, there is a need for a general parameter study of possible lunar trajectories covering a wide range in insertion conditions. Presented herein are the results of such a study.

The restricted two-body orbit equations were employed to calculate two-dimensional (coplanar) lunar ballistic trajectories. A sphere of influence was assumed to exist about the earth and about the moon such that the attraction of each body on the vehicle could be treated separately by use of the two-body equations. The earth and moon were taken as point masses, and the moon was considered to be in a circular orbit.

The primary results of the study are presented in the form of charts from which approximate insertion conditions (velocity, radius vector or altitude, flight-path angle, and lunar lead angle or firing time) can be selected for specified lunar ballistic missions. Data are included for a wide range of lunar lead angles and for a range of vehicle insertion velocities up to 80,000 ft/sec. Although portions of these ranges are impractical from a standpoint of trip time, trajectory sensitivity to insertion error, or performance capability,

the data are included to show the scope of possible lunar trajectories.

Where applicable, the data are normalized to show effects of the various insertion parameters on trip time, lunar miss distance, and other results.

ASSUMPTIONS AND METHOD

The charts presented in this paper are based on a number of assumptions. One basic assumption is that a sphere of influence exists about each attracting body. It is further assumed that the lunar trajectory can be divided into two parts as follows:

(1) In one part, the motion is inside the sphere of influence of the earth and outside the sphere of influence of the moon. (Within this sphere the effect of the moon is neglected.)

(2) In the other part, the motion is inside the sphere of influence of the moon. (Within this sphere the effect of the earth is neglected.)

Both parts of the trajectory are calculated by means of the restricted two-body orbit equations. Part (1) includes the trajectory for both the approach to and the return from the sphere of influence of the moon. For this part, the geocentric (earth) coordinate system of axes is used. At the point where the vehicle enters the sphere of influence of the moon the trajectory parameters are converted to the selenocentric (moon) coordinate system. Trajectories which pass outside the sphere of influence of the earth before passing through the sphere of influence of the moon are not considered. All trajectories are calculated for insertion in a counterclockwise direction (looking down on the north pole of the earth). This direction refers to an eastward launch.

The motion inside the sphere of influence of the earth can be elliptic, parabolic, or hyperbolic depending on the insertion velocity. The motion inside the sphere of influence of the moon is always hyperbolic when expressed in selenocentric coordinates. This fact is shown in references 1 and 2 as is the basic method used herein for calculating the trajectories.

The other basic assumptions used in these calculations are:

(1) The earth and moon are homogeneous spheres and are considered as point masses.

(2) The moon revolves about the center of the earth in a circular orbit. Average values for the orbital radius and angular velocity of the moon are taken unless otherwise specified.

(3) The effects of the sun and all other perturbing bodies are neglected.

(4) The trajectory of the vehicle lies in the plane described by the rotation of the moon about the earth.

Definitions of the symbols used herein are given in appendix A. The equations of motion used are presented in detail in appendix B. The method used for determining the radii of the spheres of influence of the moon and earth is presented in appendix C. A limited comparison of the results with those obtained from the use of the classic restricted three-body equations of motion (for both the two-dimensional and three-dimensional case) is presented subsequently.

RANGE OF PARAMETERS

The insertion parameters varied for this study were *inertial velocity*, *inertial flight-path angle*, distance from the center of the earth, and the lunar lead angle. Six different insertion radii were studied ranging from 4,050 to 5,000 statute miles. If the radius of the earth is assumed to be 3,960 statute miles, this range corresponds to altitudes of 90 to 1,040 statute miles. A large number of insertion velocities were examined for each insertion radius in order to determine representative charts. Seven insertion flight-path angles (0°, 4°, 10°, 14°, 20°, 40°, and 60°) were studied for each velocity. Insertion velocities varied from the minimum value required to reach the lunar sphere of influence to 80,000 ft/sec. For each combination of radius, velocity, and flight-path angle the lunar lead angle τ was varied in increments of 1°, and all possible values were covered which resulted in ballistic trajectories that entered the lunar sphere of influence. The ranges of insertion conditions studied included a relatively wide scope of possible lunar trajectories, even though it was recognized that many of the trajectories would ordinarily be impractical in regard to trip time, performance capability, or sensitivity of end conditions to insertion errors.

Examples of some minimum velocity requirements for certain values of insertion radius $r_{e,1}$ are shown in table I. The velocities required for specific apogee distances (the gravitational attraction of the moon being neglected) and the escape velocities are given. Note that the in-

TABLE I.—VELOCITIES REQUIRED FOR SPECIFIC APOGEE DISTANCES WITH GRAVITATIONAL ATTRACTION OF MOON NEGLECTED

[Values are based on moon rotating in a circular orbit about the earth at an average radius and rotational velocity]

Requirement	Velocity, ft/sec, for $r_{e,1}$ of—					
	4,050 statute miles	4,100 statute miles	4,200 statute miles	4,300 statute miles	4,500 statute miles	5,000 statute miles
For $\gamma_{e,1}=0°$, minimum insertion velocity to reach near side of lunar sphere of influence ($r_e=D-r_m*=203,076$ statute miles)	35, 928	35, 704	35, 268	34, 847	34, 048	32, 262
For $\gamma_{e,1}=0°$, minimum insertion velocity to reach center of moon ($r_e=D=238,857$ statute miles)	35, 981	35, 757	35, 322	34, 902	34, 103	32, 320
For $\gamma_{e,1}=0°$, minimum insertion velocity to reach far side of lunar sphere of influence ($r_e=D+r_m*=274,638$ statute miles)	36, 020	35, 797	35, 361	34, 941	34, 145	32, 363
Minimum insertion velocity to reach boundary of terrestrial sphere of influence ($r_e=r_e*=502,000$ statute miles)	36, 139	35, 916	35, 483	35, 064	34, 269	32, 495
Escape velocity from earth	36, 285	36, 063	35, 631	35, 214	34, 423	32, 656

sertion velocities in the first three rows pertain to insertion flight-path angles of 0°. Slightly lower velocity values (1 to 5 ft/sec lower) are required for larger flight-path angles.

RESULTS AND DISCUSSION

The primary results are presented in the form of charts from which approximate insertion conditions (velocity, radius vector or altitude, flight-path angle, and lunar lead angle or firing time) can be chosen for specified lunar missions. The values of insertion conditions obtained from these charts are based on simple equations of motion and are considered as approximations to those actually required for performing any specific lunar mission. These approximations are generally adequate for studies in which the more sophisticated equations of motion are used for simulating lunar trajectories. Trends (such as effects of errors in the insertion conditions on the lunar miss distance and trip time) are not discussed herein, as they have been widely discussed in previous publications (for example, refs. 3 to 7).

LUNAR APPROACH TRAJECTORIES

Impact boundaries.—The variation of insertion velocity with lead angle for lunar impacts is presented in figure 1 for each of the six insertion radii investigated and for a range of flight-path angles. The region bounded by the curves for a particular insertion flight-path angle includes the combinations of insertion velocity and lead angle which would result in a lunar impact. A locus of points through the middle of the region represents insertion conditions for lunar dead-center hits (trajectories which pass through the center of the moon). As indicated in the figure, the direction of vehicle motion with respect to the moon prior to impact is clockwise (CW) for insertion conditions near the upper boundary and counterclockwise (CCW) for insertion conditions near the lower boundary.

Each of the curves shown in figure 1 has a minimum value, which in effect separates the ensuing trajectories into two broad categories. The insertion conditions given by the part of the curve to the right of the minimum velocity for impact yield ballistic trajectories which impact on the moon while the vehicle is moving away from the earth. The part of the curve to the left represents ballistic trajectories which impact on the moon while the vehicle is moving toward the earth after having reached apogee. This left part is limited by the velocity (not shown in fig. 1) since trajectories having an apogee distance beyond the sphere of influence of the earth may result in orbits about the sun. (See table I for minimum insertion velocity to reach the boundary of the sphere of influence of the earth.) To the left of the minimum-velocity point on the curve,

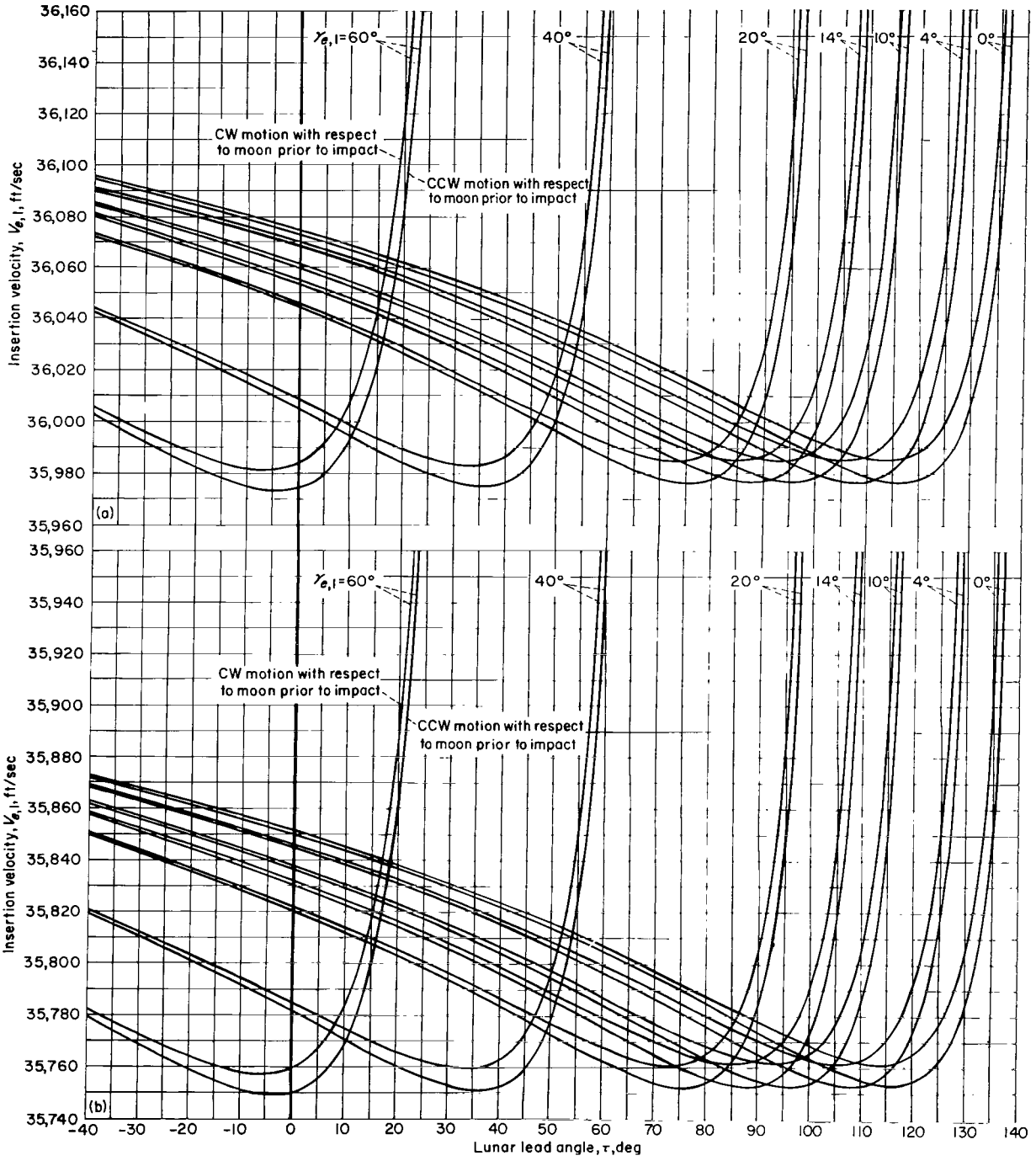

(a) $r_{e,1}$=4,050 statute miles.
(b) $r_{e,1}$=4,100 statute miles.

FIGURE 1.—Boundaries of insertion conditions for lunar impact.

the trajectories tend to become impractical as the lead angle is decreased because of increased trip time and greater sensitivity to insertion-velocity error; to the right of the minimum, the trajectories become sensitive to lead-angle error as the velocity increases.

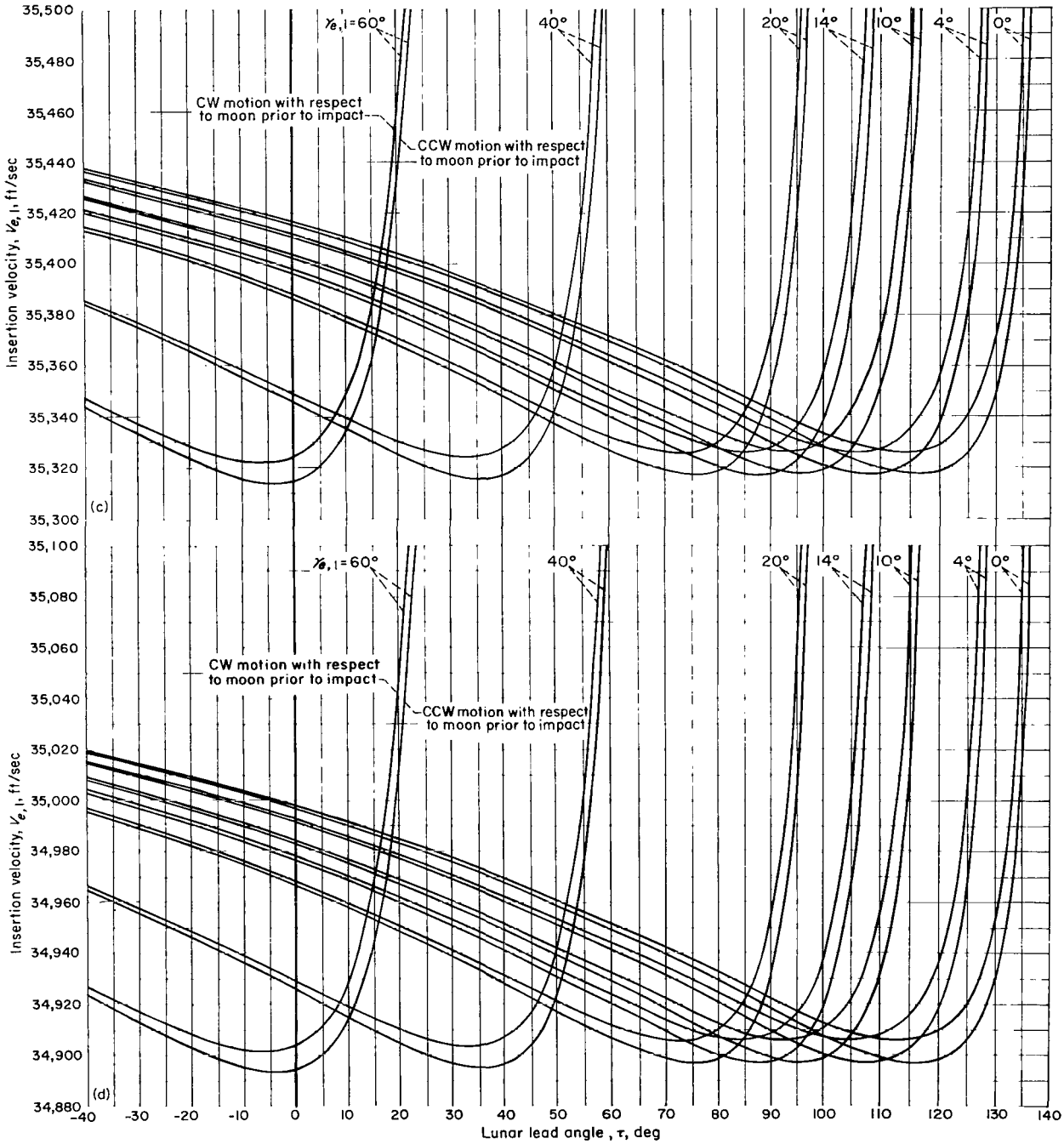

(c) $r_{e,1}$=4,200 statute miles.
(d) $r_{e,1}$=4,300 statute miles.

FIGURE 1.—Continued.

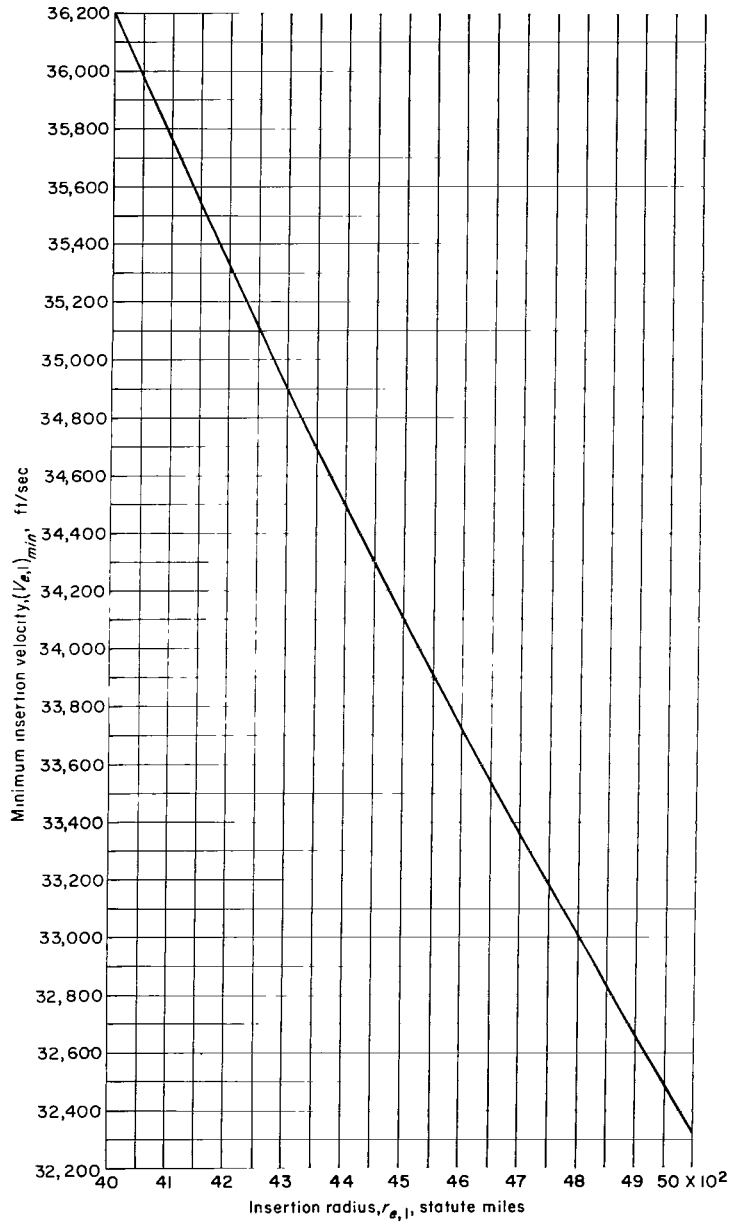

$\gamma_{e,1}$, deg	$(V_{e,1})_{min}$, ft/sec, for $r_{e,1}$, statute miles, of—					
	4,050	4,100	4,200	4,300	4,500	5,000
0	35, 977	35, 753	35, 318	34, 897	34, 099	32, 315
10	35, 976	35, 753	35, 317	34, 897	34, 099	32, 315
20	35, 976	35, 752	35, 317	34, 896	34, 098	32, 314
40	35, 975	35, 751	35, 315	34, 895	34, 097	32, 312
60	35, 973	35, 749	35, 314	34, 893	34, 094	32, 311

FIGURE 2.—Minimum insertion velocity required for lunar impact for the range of insertion radii studied. Insertion flight-path angle $\gamma_{e,1}=0°$ to 60°.

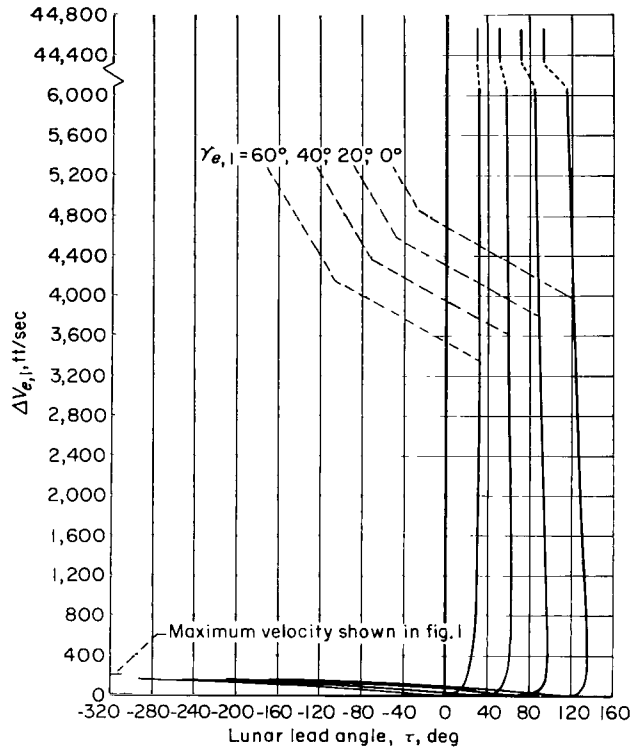

FIGURE 3.—Insertion requirements for lunar dead-center hits. Insertion radius $r_{e,1}$=4,050 to 5,000 statute miles.

Below this curve the motion is always counterclockwise. The vehicle will revolve around the far side of the moon only for trajectories in which the vehicle motion in the lunar sphere of influence is clockwise with respect to the moon. It can be noted by the sketches that in most cases the motion of the vehicle about the earth on return is in a counterclockwise direction. The motion can be in a clockwise direction for trajectories 2 and 7 only (regions 2 and 7 in the upper plot). More comprehensive data on the direction of the vehicle motion about the earth on return are included in a subsequent figure.

In figure 7 data of figures 4(d) and 4(j) are shown in normalized form for a flight-path angle of 40°. Shown in figure 7(a) is the quantity $\tau-\tau_H$, the difference between lead angle required for a given miss distance and that required for a dead-center hit, plotted against lunar miss distance for given values of incremental insertion velocity $\Delta V_{e,1}$. These data apply only to trajectories for which perilune occurs while the vehicle is moving away from the earth (those of part A of fig. 5). It may be noted in figure 7(a) that the data for insertion radii of 4,100 and 4,500 statute miles nearly coincide and are essentially linear for a given incremental insertion velocity for miss distances greater than the radius of the moon (1,080 statute miles). The slope of the line, however, is different for positive and negative values of the quantity $\tau-\tau_H$. Plots of this type for other flight-path angles would indicate results similar to those shown in figure 7(a).

Similar results (fig. 7(b)) were obtained for trajectories where perilune occurs while the vehicle is moving toward the earth (those of part B of fig. 5). In this case the quantity $V_{e,1}-(V_{e,1})_H$, the difference between insertion velocity required for a given miss distance and that required for a dead-center hit, is plotted against lunar miss distance for given lunar lead angles. (This velocity difference should not be confused with the $\Delta V_{e,1}$ term used elsewhere in this study.)

On the basis of the comparisons for the two insertion radii shown in figure 7, the data given in figures 4(a) to 4(e) for an insertion radius of 4,100 statute miles can be applied over a wide range of insertion radii (at least up to 4,500 statute miles). This extrapolation can be made by using plots such as those shown in figure 7 for various lunar lead angles τ or incremental insertion velocities $\Delta V_{e,1}$ in conjunction with the data given in figure 1. The resulting plots will indicate, to a good approximation, insertion requirements for any desired lunar miss distance for a particular insertion altitude and flight-path angle.

Velocity at closest approach to moon.—The variation of vehicle velocity at perilune with perilune distance $r_{m,p}$ is shown in figure 8 for several incremental insertion velocities. Also shown is the minimum perilune velocity possible for ballistic trajectories and the velocity necessary to establish a circular orbit about the moon at a given radius. The data in figure 8 are separated according to the direction of vehicle motion with respect to the moon. In addition, the open symbols correspond to insertion conditions for the trajectories of part A of figure 5 (perilune occurs while vehicle is moving away from the earth). The solid symbols correspond to trajectories of part B of figure 5. Data for the trajectories of part B are not shown for $\Delta V_{e,1}$=178 ft/sec as this value exceeds the permissible velocity for remaining within the sphere of influence of the earth.

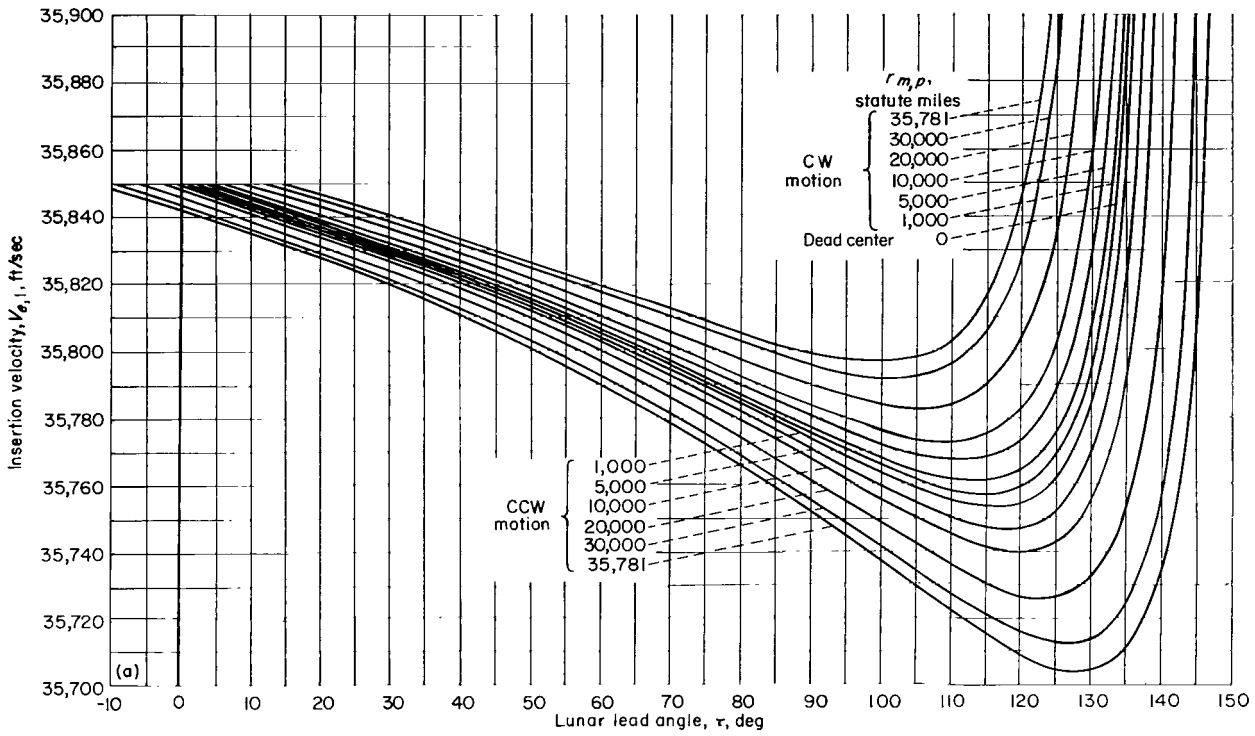

(a) $r_{e,1}=4{,}100$ statute miles; $\gamma_{e,1}=0°$.

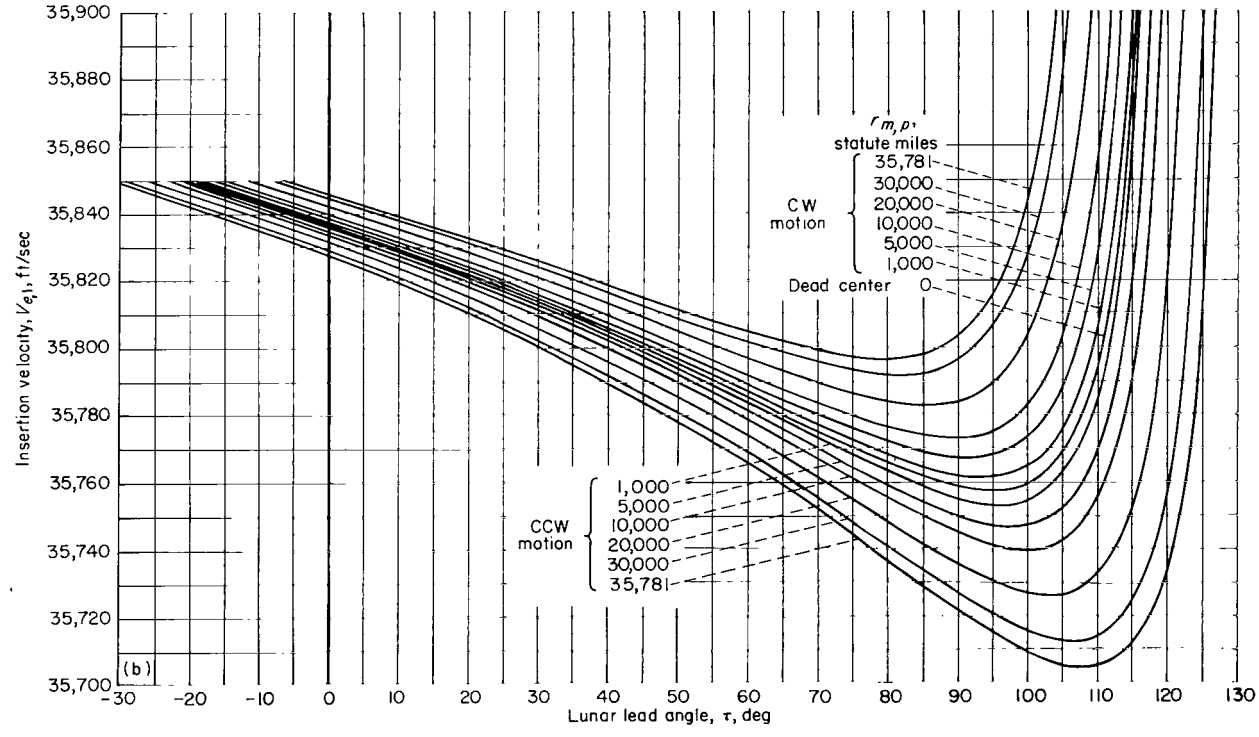

(b) $r_{e,1}=4{,}100$ statute miles; $\gamma_{e,1}=10°$.

FIGURE 4.—Insertion conditions required to obtain a given lunar miss distance for clockwise (CW) motion and counterclockwise (CCW) motion of the vehicle with respect to the moon.

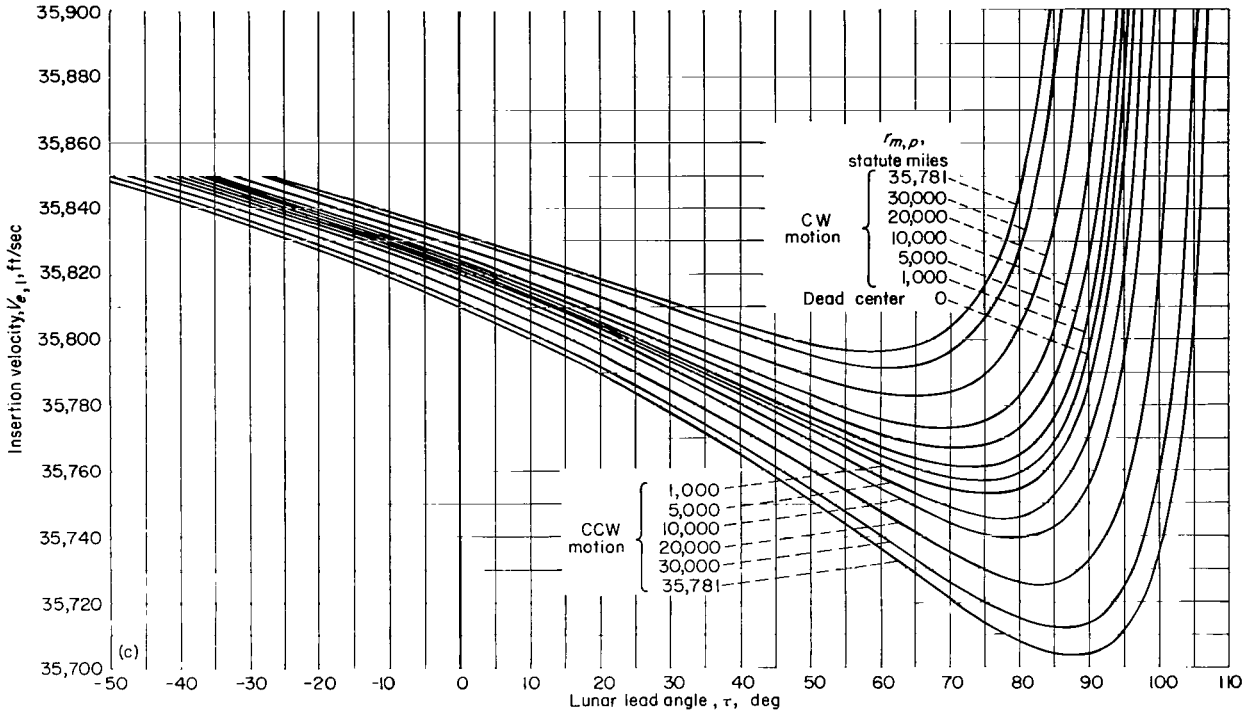

(c) $r_{e,1}=4{,}100$ statute miles; $\gamma_{e,1}=20°$.

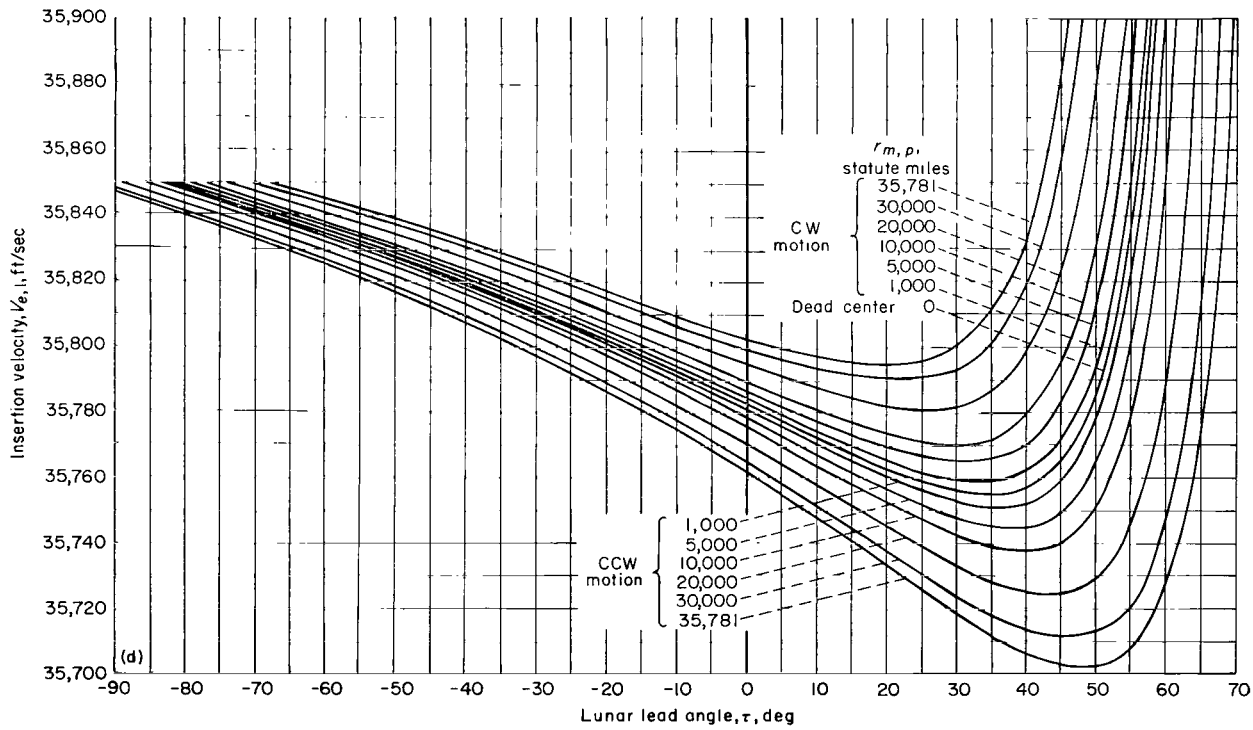

(d) $r_{e,1}=4{,}100$ statute miles; $\gamma_{e,1}=40°$.

FIGURE 4.—Continued.

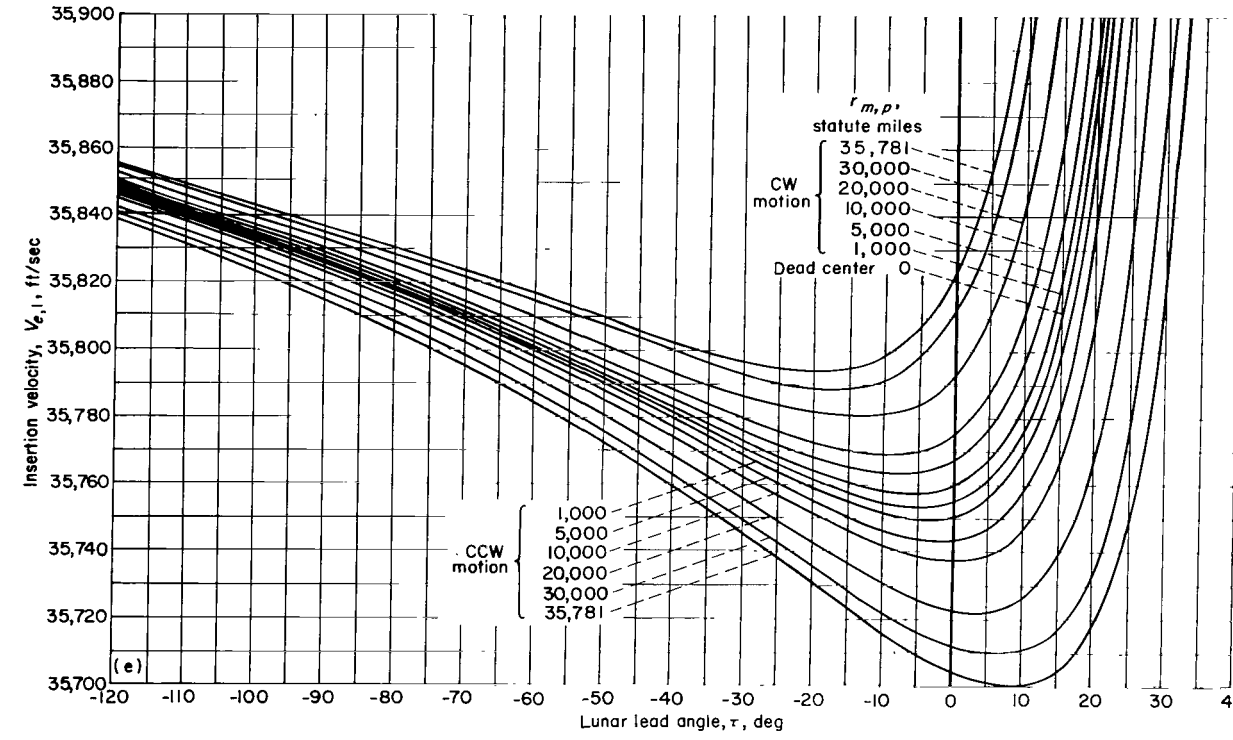

(e) $r_{e,1}$=4,100 statute miles; $\gamma_{e,1}$=60°.

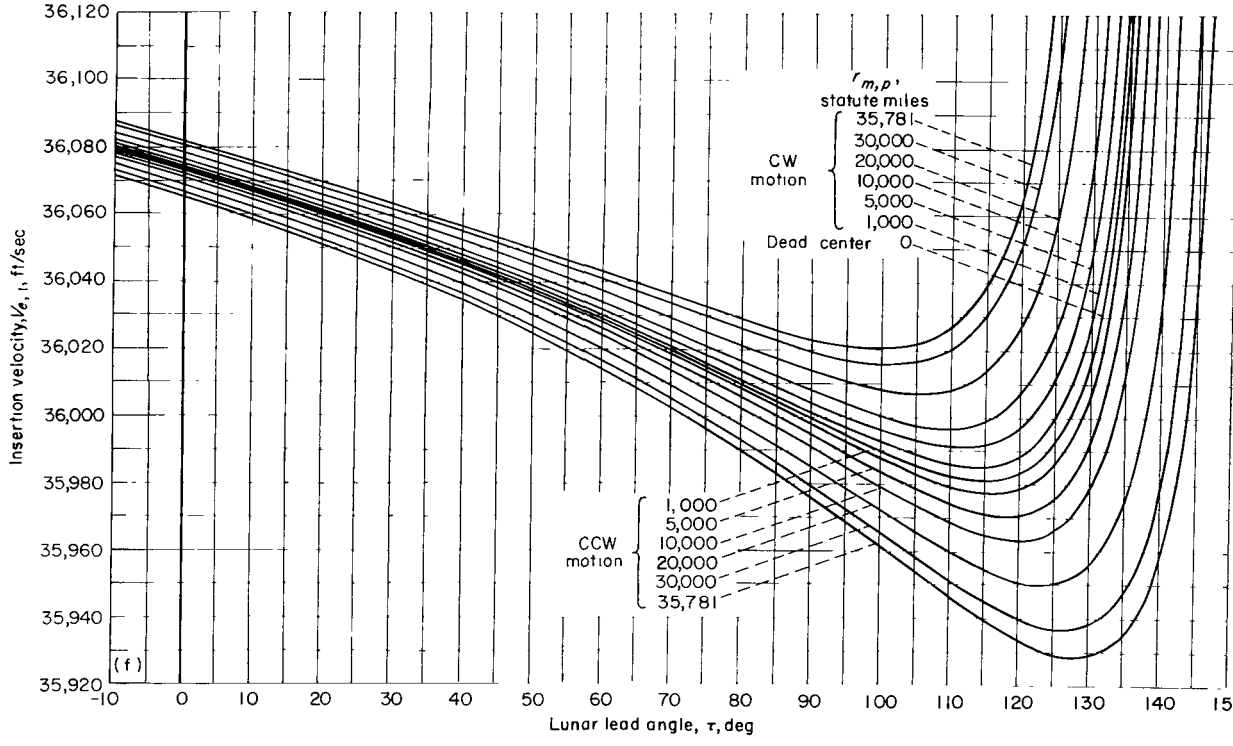

(f) $r_{e,1}$=4,050 statute miles; $\gamma_{e,1}$=0°.

FIGURE 4.—Continued.

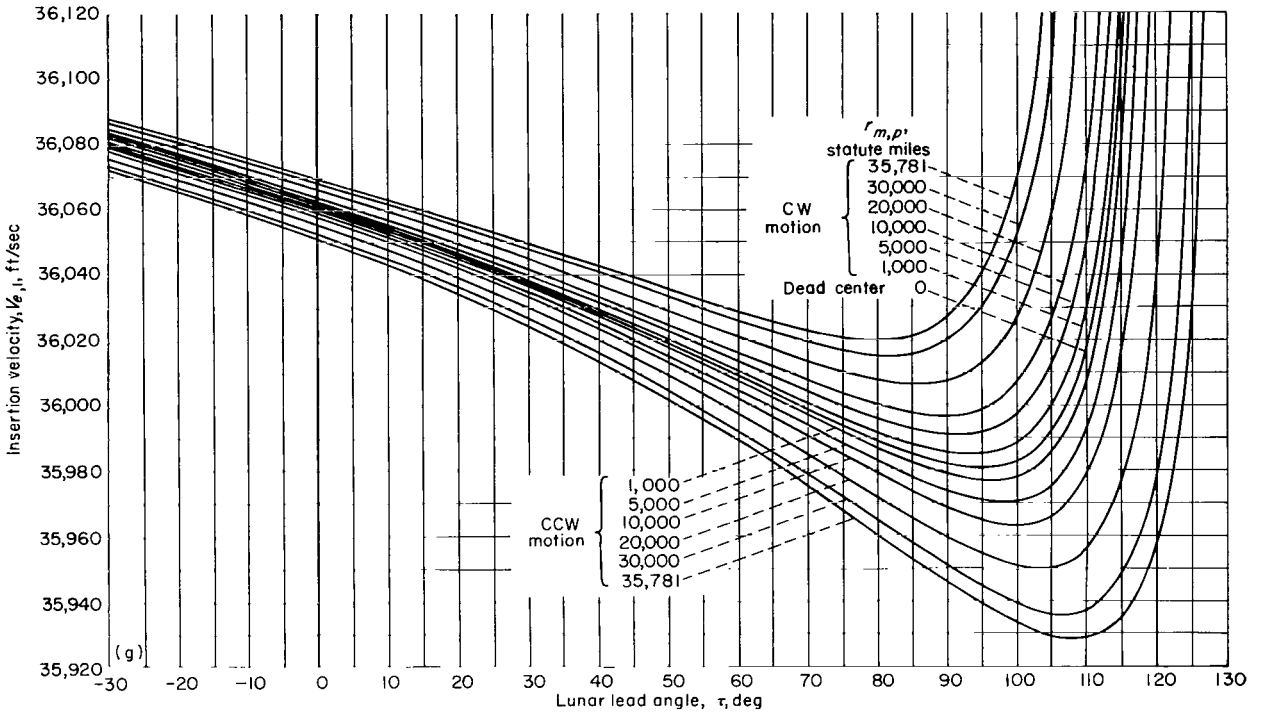

(g) $r_{e,1}=4{,}050$ statute miles; $\gamma_{e,1}=10°$.

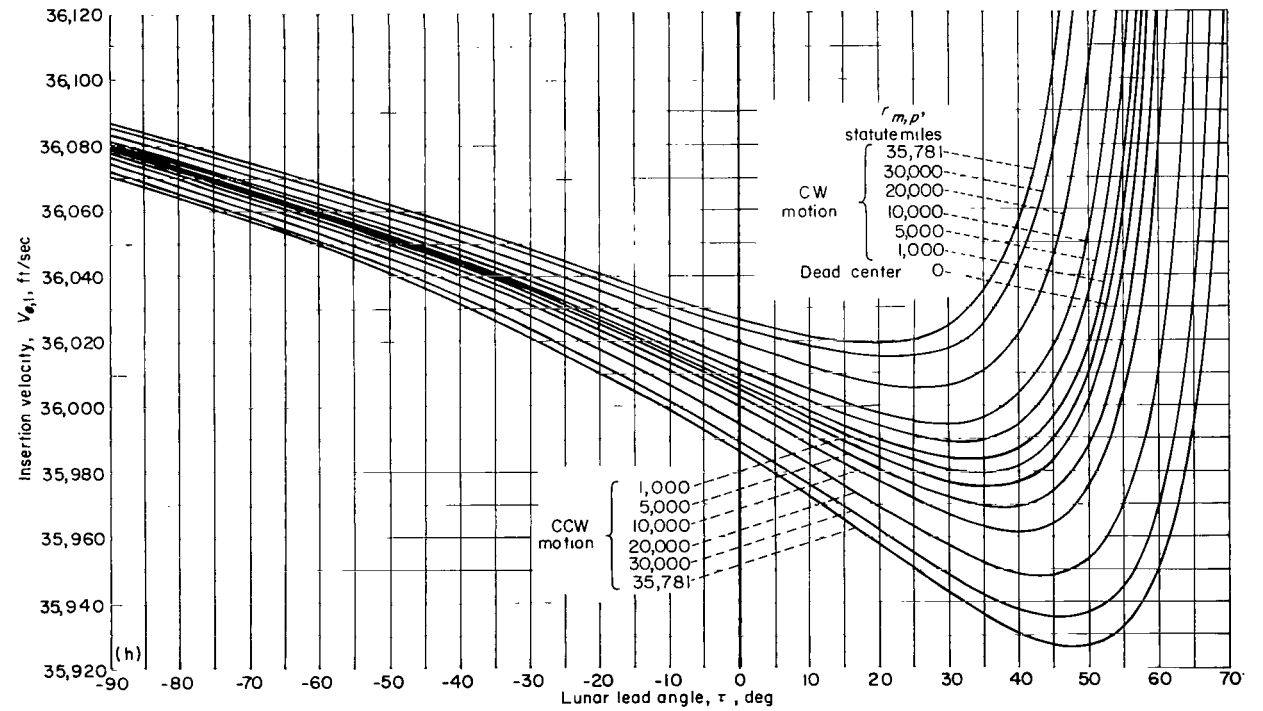

(h) $r_{e,1}=4{,}050$ statute miles; $\gamma_{e,1}=40°$.

FIGURE 4.—Continued.

670951—63——3

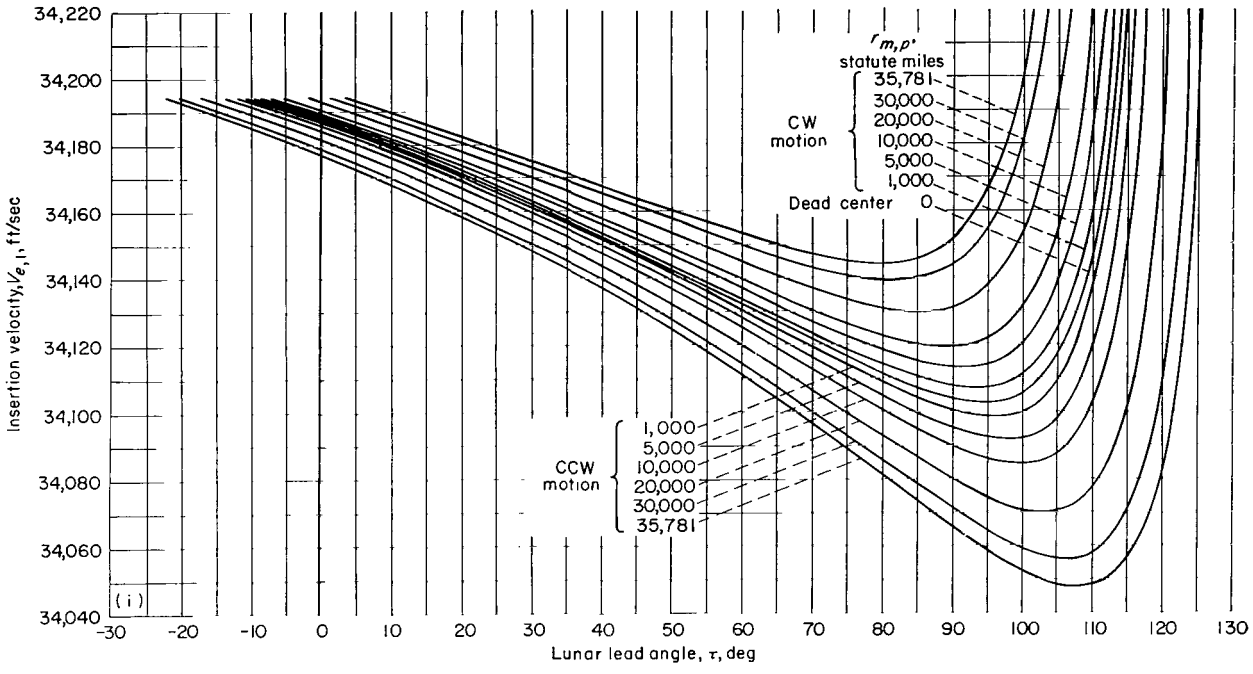

(i) $r_{e,1}$=4,500 statute miles; $\gamma_{e,1}$=10°.

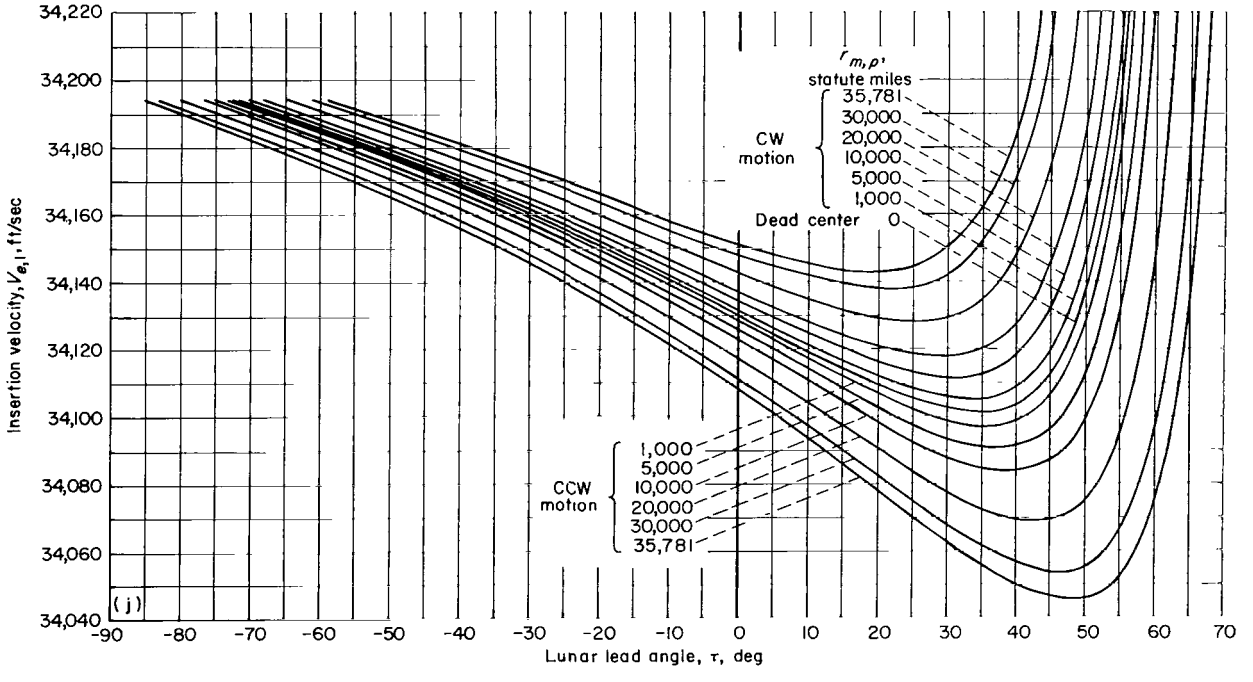

(j) $r_{e,1}$=4,500 statute miles; $\gamma_{e,1}$=40°.

FIGURE 4.—Concluded.

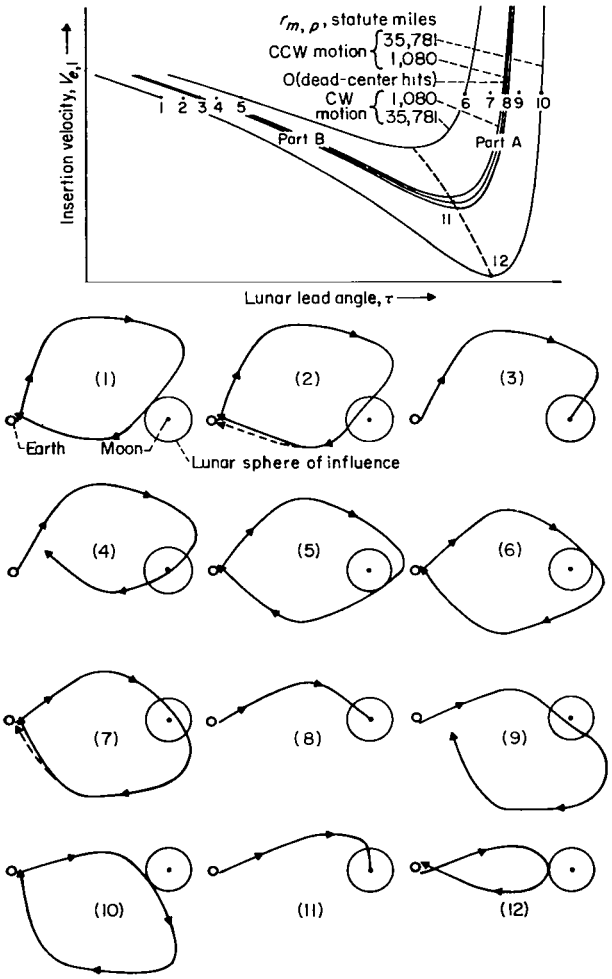

FIGURE 5.—Representative plots of lunar trajectories in rotating axis system for various combinations of insertion conditions.

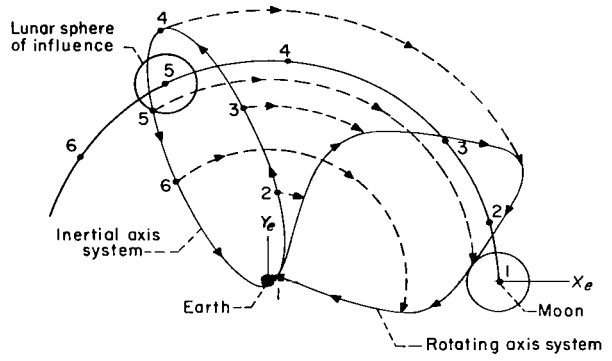

FIGURE 6.—Example showing transformation of trajectory in inertial axis system to rotating axis system (trajectory (1) of fig. 5).

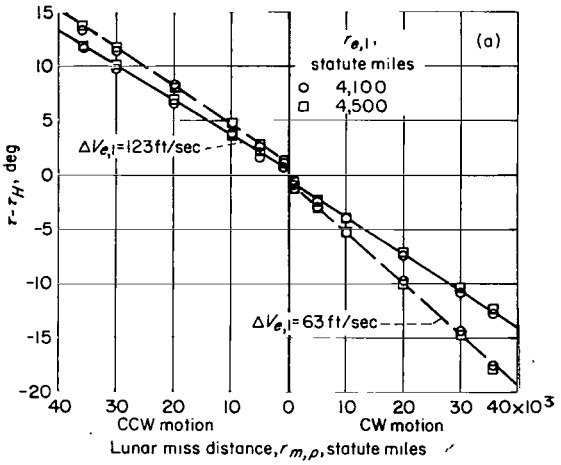

(a) Lunar-lead-angle difference plotted against lunar miss distance for constant insertion velocity.

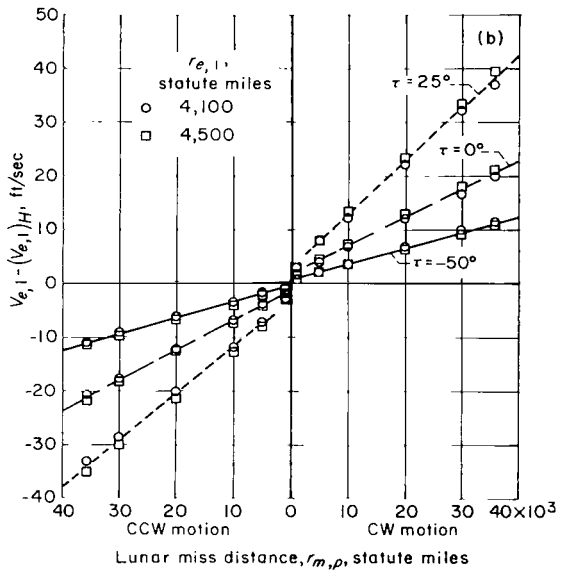

(b) Insertion-velocity difference plotted against lunar miss distance for constant lunar lead angle.

FIGURE 7.—Variation of lunar miss distance with insertion velocity and lunar lead angle. Insertion flight-path angle $\gamma_{e,1}=40°$.

In figure 8 the data for $\Delta V_{e,1}=97$ ft/sec are shown for two insertion radii and two insertion flight-path angles. It can be seen that perilune velocity is essentially unaffected by these two variables. Also, it can be noted that for a given $r_{m,p}$ there is only a small difference in

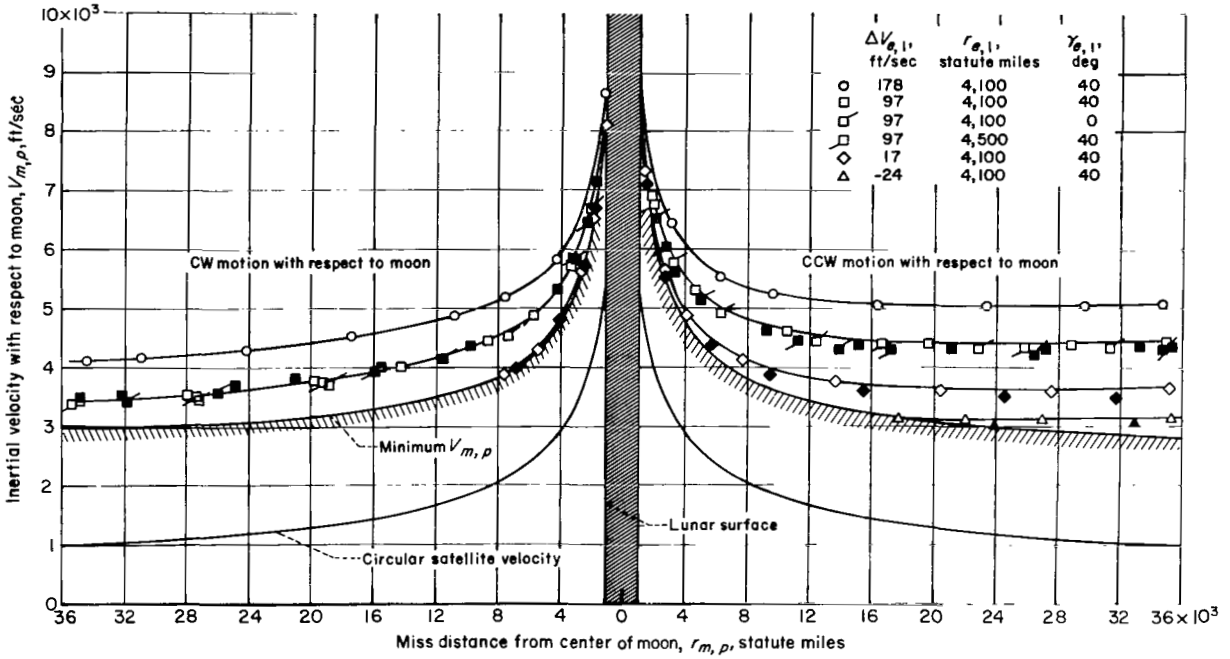

FIGURE 8.—Vehicle velocity at perilune of ballistic trajectories. Open symbols (or solid symbols) represent trajectories where perilune is reached while vehicle is moving away from (or toward) earth.

perilune velocity (approximately 100 ft/sec) between the data of parts A and B of figure 5. It is of interest to note that for counterclockwise motion, perilune velocity is relatively constant at values of $r_{m,p}$ greater than about 16,000 statute miles. Also, the intersections of the curves with the lunar-surface line represent the impact velocities attained with lunar ballistic trajectories.

Longitude limits of lunar impact.—For lunar ballistic trajectories designed to impact on the moon, the impact longitude is of interest. In figure 9 the longitude limits of lunar impact are plotted against incremental insertion velocity $\Delta V_{e,1}$ for several insertion flight-path angles and insertion radii. Shown as a dashed line is the impact longitude for trajectories designed to intersect the center of the moon (dead-center hit). In the figure, lunar longitude is measured clockwise in the plane of motion (looking down on north pole of moon). The location of 0° longitude for the moon is the intersection of the lunar surface with a line joining the centers of the earth and moon.

The boundaries shown in figure 9(a) represent the longitude limits for trajectories which impact on the moon while the vehicle is moving away from the earth. (These trajectories correspond to insertion conditions given by part A of fig. 5.) For example, for $\Delta V_{e,1}=100$ ft/sec, any impact longitude from about −90° to 185° (measured clockwise) can be attained, depending on the

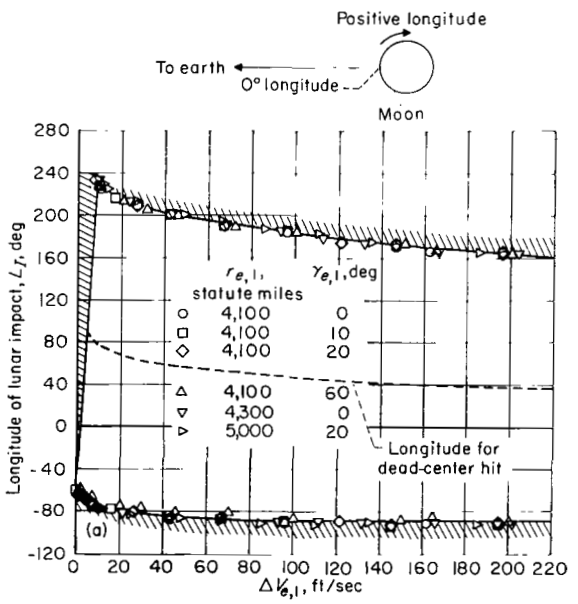

(a) Impact while vehicle is moving away from earth.

FIGURE 9.—Limits of lunar longitude attainable for lunar impacts of ballistic trajectories.

lead angle. At velocities above those shown in figure 9(a), the lower curve remains at a longitude of −90° while the top curve approaches 90°.

The boundaries shown in figure 9(b) represent longitude limits for trajectories which impact on the moon while the vehicle is moving toward the earth after having reached apogee (part B of fig. 5). In figure 9(b) the curves for given values of $r_{e,1}$ and $\gamma_{e,1}$ will terminate at the value of $\Delta V_{e,1}$ corresponding to the minimum insertion velocity to reach the boundary of the sphere of influence of the earth. (See table I.) The value of $\Delta V_{e,1}$ at this maximum velocity changes somewhat with insertion flight-path angle and/or insertion radius. For example, at $r_{e,1}$=4,100 statute miles and $\gamma_{e,1}$=0°, the maximum value of $\Delta V_{e,1}$ is 163 ft/sec; at $r_{e,1}$=5,000 statute miles and $\gamma_{e,1}$=20°, the maximum value of $\Delta V_{e,1}$ is 181 ft/sec.

The data in figure 9 indicate that neither insertion flight-path angle nor insertion radius has a significant effect on the impact longitude limits. For lunar ballistic impacts while the vehicle is moving away from the earth (fig. 9(a)), longitudes from about 230° to 270° (measured clockwise) are not attainable at any velocity. In figure 9(b) it is seen that longitudes from about 270° to 300° (or −60°) cannot be attained with ballistic trajectories which impact while the vehicle is moving toward the earth.

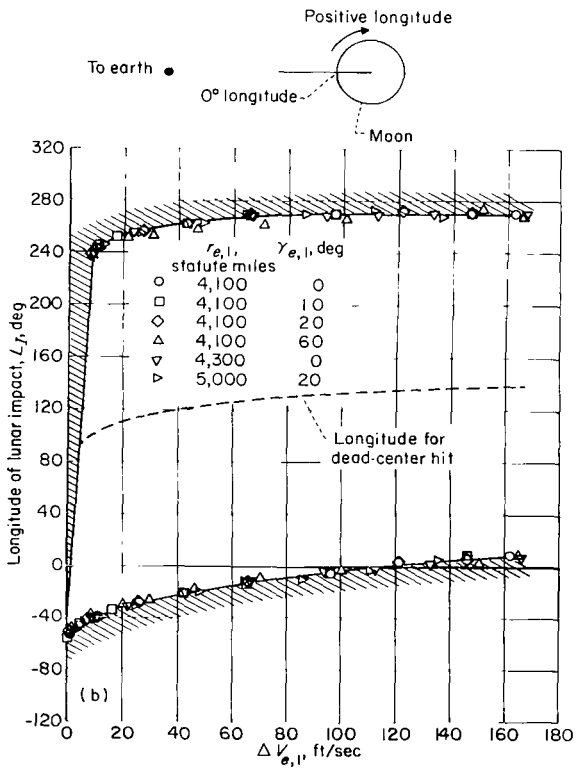

(b) Impact while vehicle is moving toward earth.

FIGURE 9.—Concluded.

Longitude of closest approach to moon.—Information on the lunar longitude of perilune may be required for the various types of lunar missions. In figure 10 perilune longitudes for ballistic trajectories are plotted against miss distance for a range of incremental insertion velocities $\Delta V_{e,1}$. The data cover perilune distances $r_{m,p}$ from the lunar surface out to the boundary of the lunar sphere of influence. The data shown in figure 10(a) represent trajectories in which perilune is reached while the vehicle is moving away from the earth (part A in fig. 5). In figure 10(b) perilune is reached while the vehicle is moving toward the earth (part B of fig. 5). Data from a three-body analysis (ref. 6) are shown for two velocities for comparison with the present results. (See fig. 10(a).)

For a $\Delta V_{e,1}$ value of 41 ft/sec, data are shown for two insertion radii and two flight-path angles. These data show perilune longitude to be essentially independent of insertion radius and flight-path angle. Although its variation with insertion velocity is nonlinear, a good approximation of the perilune longitude for any given insertion velocity may be obtained by interpolation of the data in figure 10.

Included also in figure 10 are the limits for observing the vehicle at perilune. These limits show the perilune longitudes at which the vehicle is never observable from the earth as well as those at which the vehicle is observable only from limited positions on the earth. It is shown in figure 10(a) that for trajectories in which the vehicle is in clockwise motion with respect to the moon, perilune is not observable from the earth in some cases. It should be stated that these cases represent insertion conditions which are desirable from the standpoint of total trip time from insertion to return to earth. As indicated in figure 10(b) the vehicle is always observable at perilune except for near-impact cases with clockwise motion.

Trip times to closest approach to moon.—Another item of interest for lunar missions is trip

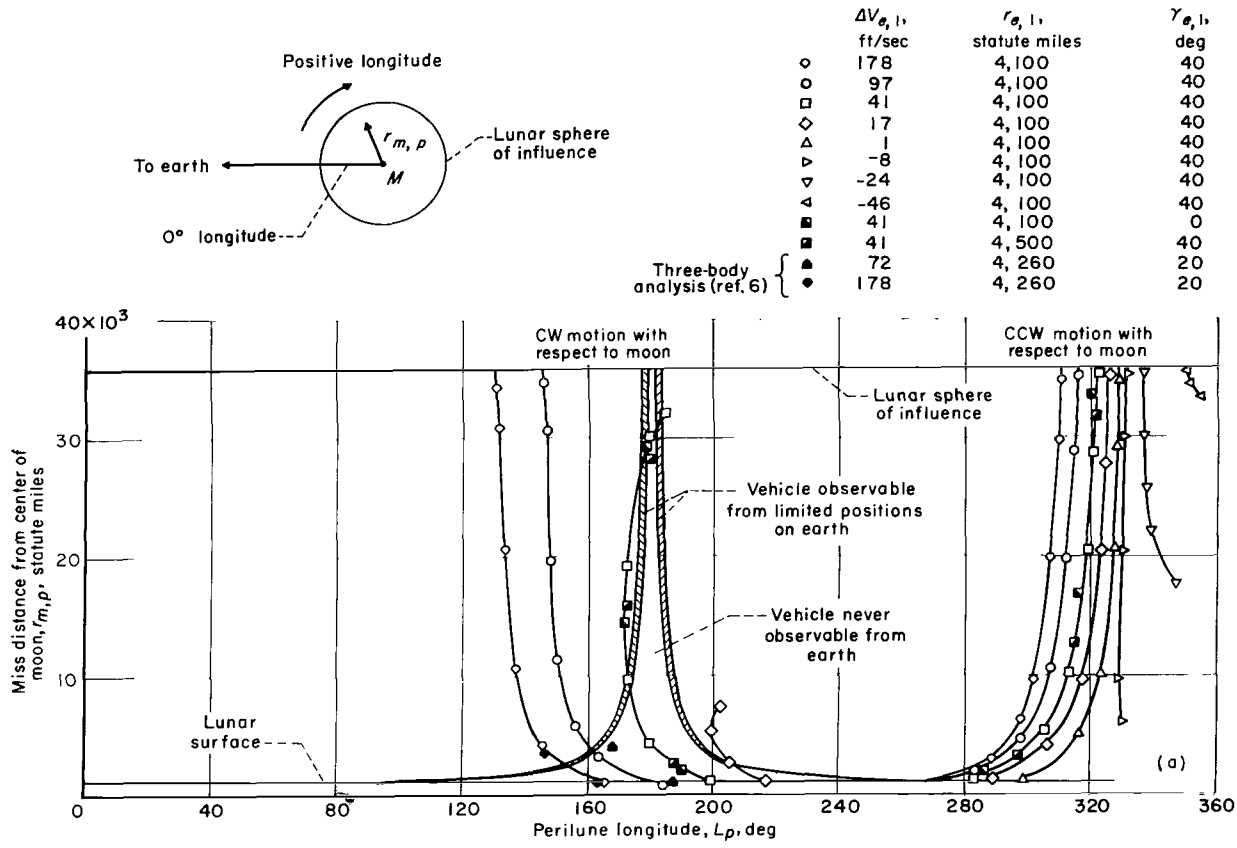

(a) Perilune reached while vehicle is moving away from earth.

FIGURE 10.—Lunar longitude for perilune of ballistic trajectories. Vehicle is observable from earth except where indicated.

time. Trip time from insertion to perilune is plotted against incremental velocity $\Delta V_{e,1}$ in figure 11. The data points represent trip times for ballistic trajectories in which perilune occurs at the boundary of the lunar sphere of influence. Values of trip time for cases in which perilune is within the lunar sphere of influence fall between the curves. Trip times for trajectories in which the perilune is at the center of the moon (dead-center hit) are indicated by the dashed lines.

The data in figure 11 are shown for two insertion radii with a different insertion flight-path angle for each radius. The vertical and horizontal scales are broken to indicate, respectively, the maximum trip time and trip time for $\Delta V_{e,1}$ =44,247 ft/sec ($V_{e,1} \approx 80{,}000$ ft/sec). The shorter trip times (lower sections of the curves) apply to part A of figure 5 whereas the longer trip times apply to part B. Long trip times associated with part B make these trajectories generally impractical.

It may be seen that shorter trip times are essentially independent of both insertion flight-path angle and insertion radius. For the longer trip times there is some deviation between the two sets of insertion conditions. It was found that for a given $\Delta V_{e,1}$ this deviation in trip time is due to the difference in insertion radius and not in flight-path angle. As previously indicated, actual insertion velocity $V_{e,1}$ decreases as insertion radius increases for any given value of incremental insertion velocity $\Delta V_{e,1}$.

EARTH RETURN TRAJECTORIES

Return to earth within a specified perigee.—For lunar missions designed to pass near the moon and return to the earth, perigee of the return trajectory is of import. Plotted in figure 12 are regions for

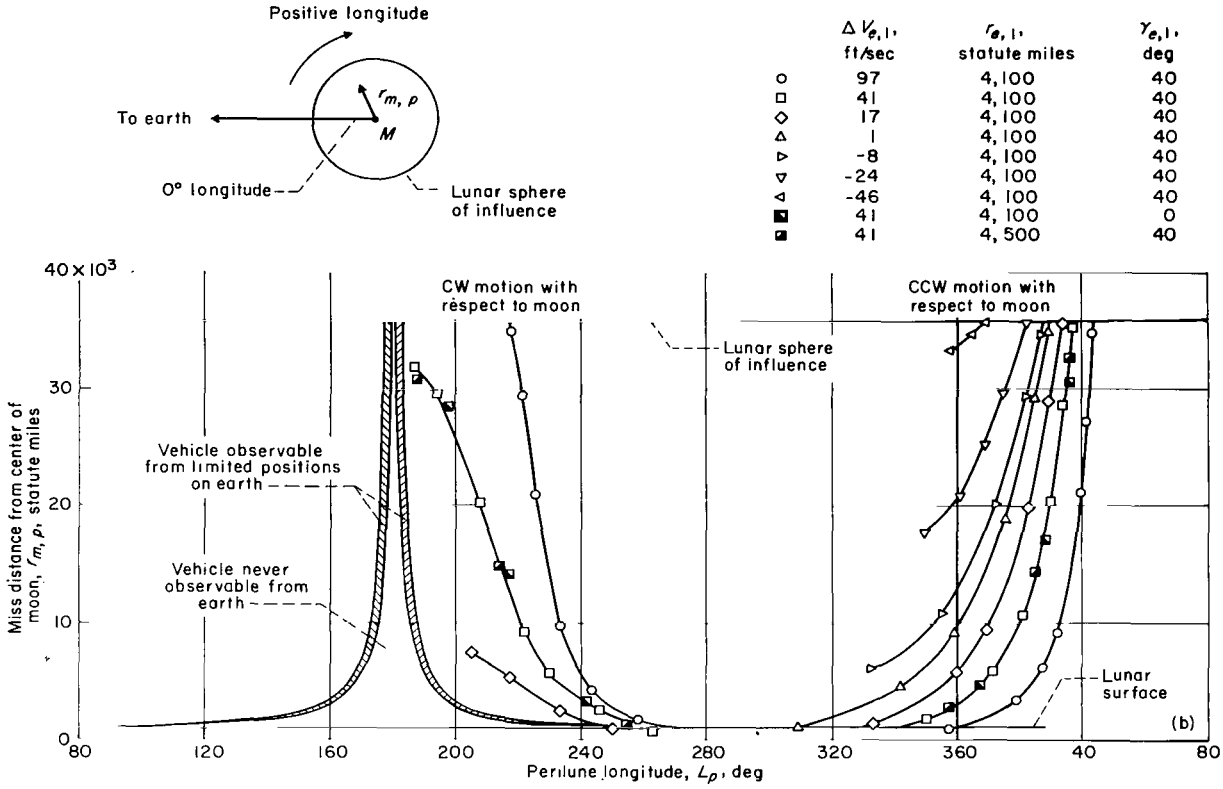

(b) Perilune reached while vehicle is moving toward earth.

FIGURE 10.—Concluded.

combinations of incremental insertion velocity $\Delta V_{e,1}$ and lead angle τ which result in a perigee radius of 4,000 statute miles or less for the return trajectory (40 statute miles or less above the assumed surface of the earth). This altitude was arbitrarily selected for illustrative purposes. The data are given for five insertion flight-path angles (0°, 10°, 20°, 40°, and 60°) and two insertion radii (4,100 and 4,500 statute miles) and apply only to trajectories which enter the lunar sphere of influence. The regions for the specified return for an insertion radius of 4,100 statute miles are between the curves faired through the circular data points. The motion of the vehicle about the earth on return will be in a counterclockwise direction except where indicated by the hatched areas. These areas are shown for an insertion radius of 4,100 statute miles. Areas for an insertion radius of 4,500 statute miles would be similar to these and in the same position relative to the square symbols. A dashed line representing the requirements for a lunar dead-center hit ($r_{e,1}$=4,100 statute miles) is shown for purposes of orientating the data in this figure with data given in figure 4.

The regions for return are not shown for the relatively high velocities. As lead angle decreases, however, the region for counterclockwise motion will terminate at the value of $\Delta V_{e,1}$ corresponding to the insertion velocity for which the apogee reaches a distance equal to the radius of the sphere of influence of the earth. (See table I.) As lead angle increases, the region for clockwise motion will terminate at a different value of $\Delta V_{e,1}$ because of the effect of passing through the lunar sphere of influence before reaching apogee.

Comparison of the data in figures 12(a) to 12(e) for the two insertion radii shows that, in most cases, insertion radius has little effect on the limits for the return regions. There are some differences due to insertion radius at the lower values of lunar lead angle (long trip times to reach perilune). Also, for the lower flight-path angles (0° to 20°), differences between the two insertion radii can be noted in each region at the lower values of $\Delta V_{e,1}$.

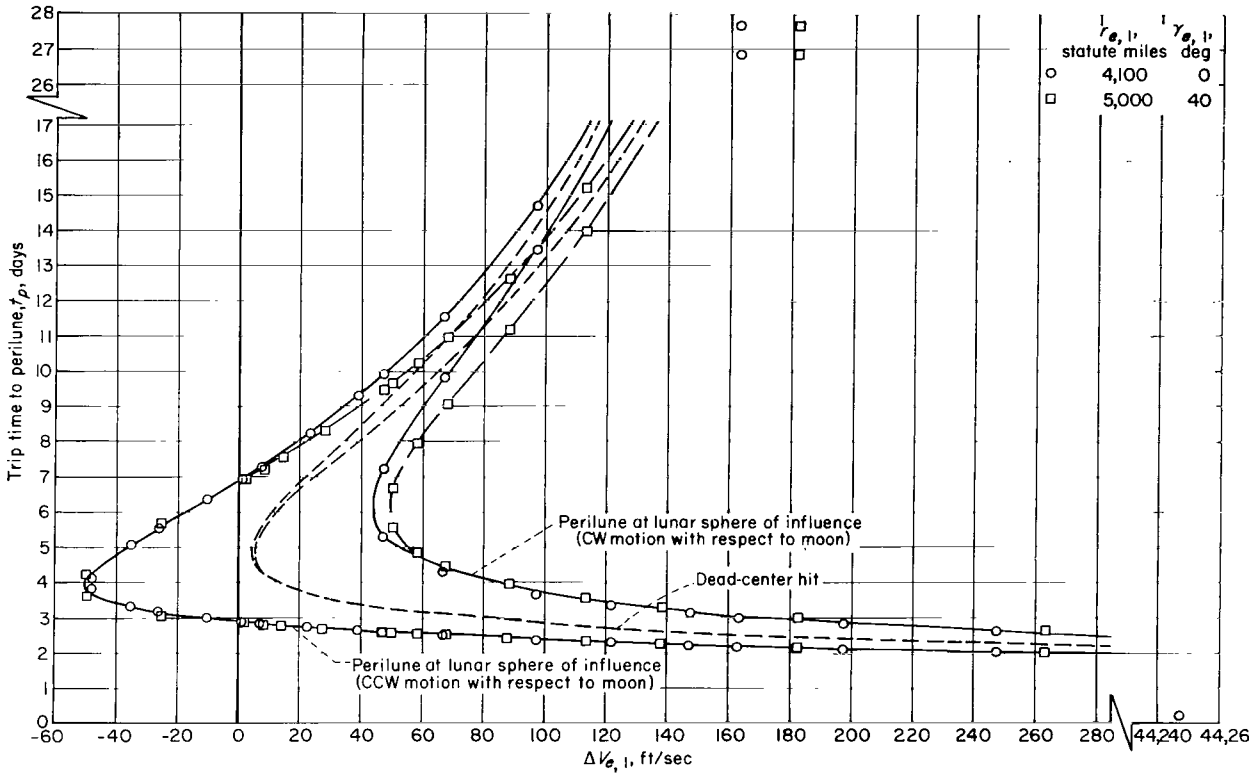
$r_{e,1}$, statute miles
$\gamma_{e,1}$, deg
4,100 0
5,000 40
Trip time to perilune, t_p, days
Perilune at lunar sphere of influence (CW motion with respect to moon)
Dead-center hit
Perilune at lunar sphere of influence (CCW motion with respect to moon)
44,240 44,260
$\Delta V_{e,1}$, ft/sec

FIGURE 11.—Variation of trip time from insertion to perilune with incremental velocity $\Delta V_{e,1}$.

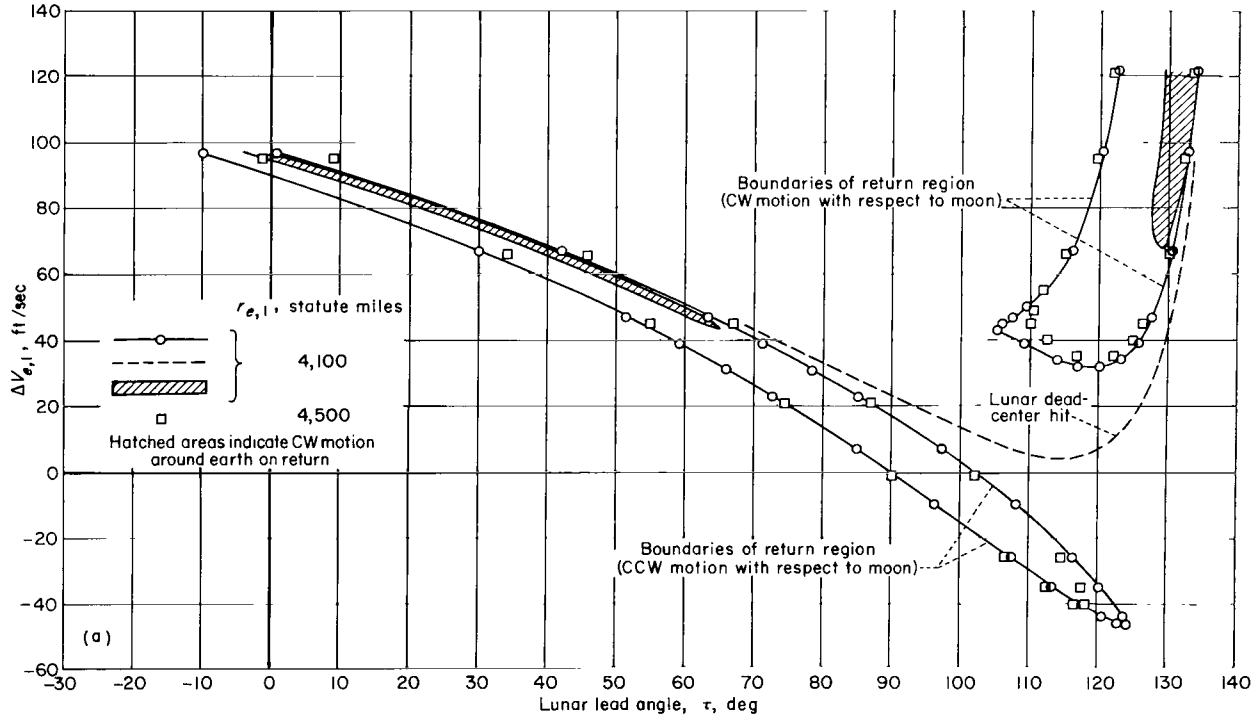
Boundaries of return region (CW motion with respect to moon)
$r_{e,1}$, statute miles
4,100
4,500
Hatched areas indicate CW motion around earth on return
Lunar dead-center hit
Boundaries of return region (CCW motion with respect to moon)
(a)
$\Delta V_{e,1}$, ft/sec
Lunar lead angle, τ, deg

(a) $\gamma_{e,1}=0°$.

FIGURE 12.—Regions of insertion conditions for return to within 40 statute miles from the surface of the earth.

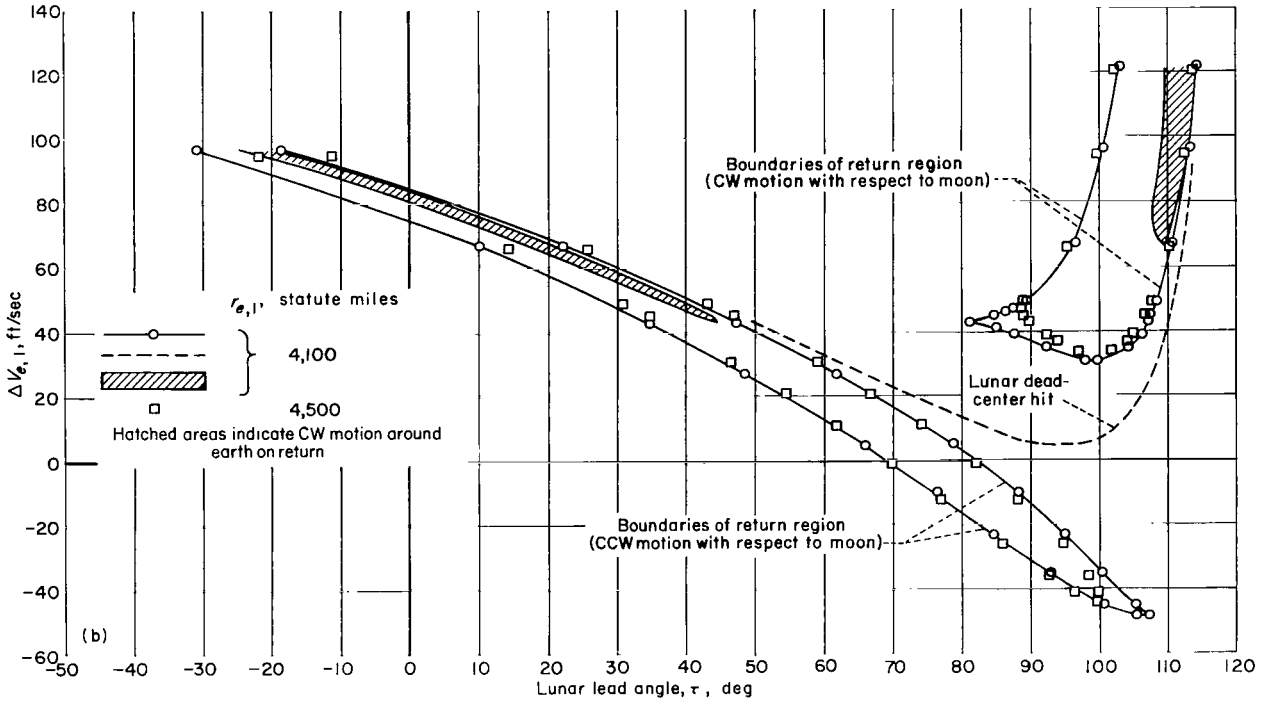
$r_{e,1}$, statute miles
4,100
4,500
Hatched areas indicate CW motion around earth on return
Boundaries of return region (CW motion with respect to moon)
Lunar dead-center hit
Boundaries of return region (CCW motion with respect to moon)
$\Delta V_{e,1}$, ft/sec
Lunar lead angle, τ, deg
(b)

(b) $\gamma_{e,1}=10°$.

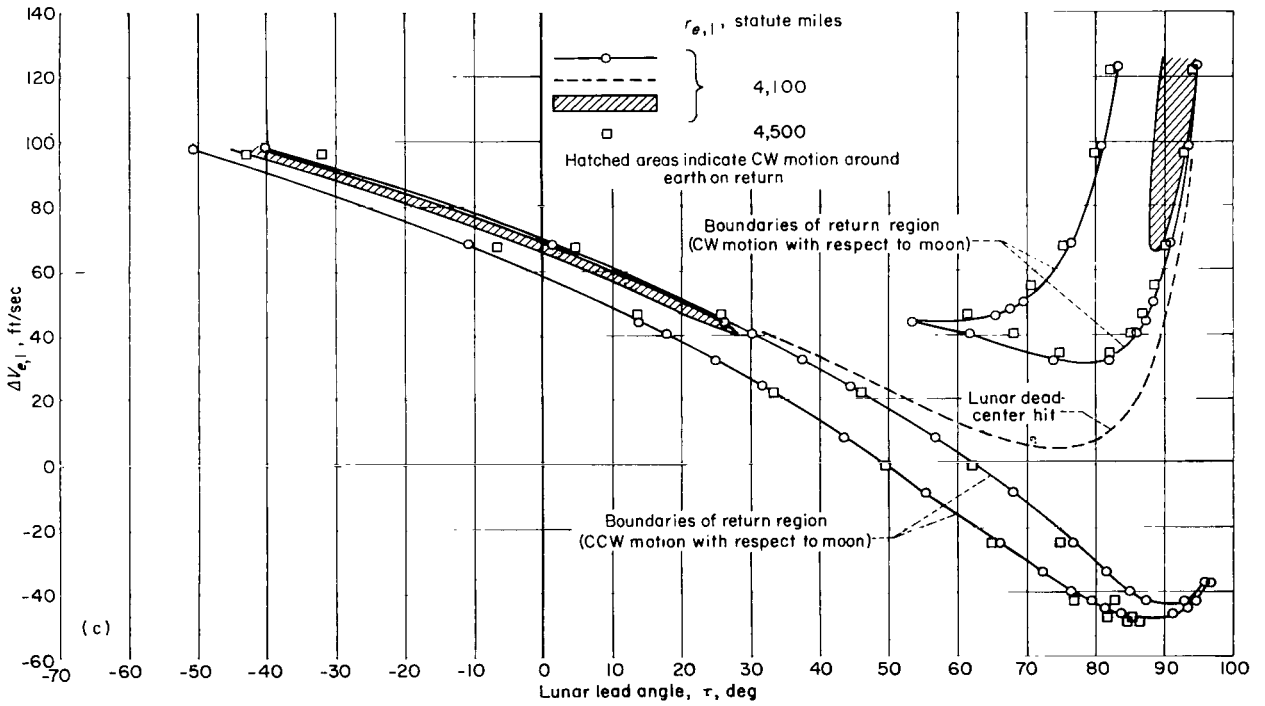
$r_{e,1}$, statute miles
4,100
4,500
Hatched areas indicate CW motion around earth on return
Boundaries of return region (CW motion with respect to moon)
Lunar dead-center hit
Boundaries of return region (CCW motion with respect to moon)
$\Delta V_{e,1}$, ft/sec
Lunar lead angle, τ, deg
(c)

(c) $\gamma_{e,1}=20°$.

FIGURE 12.—Continued.

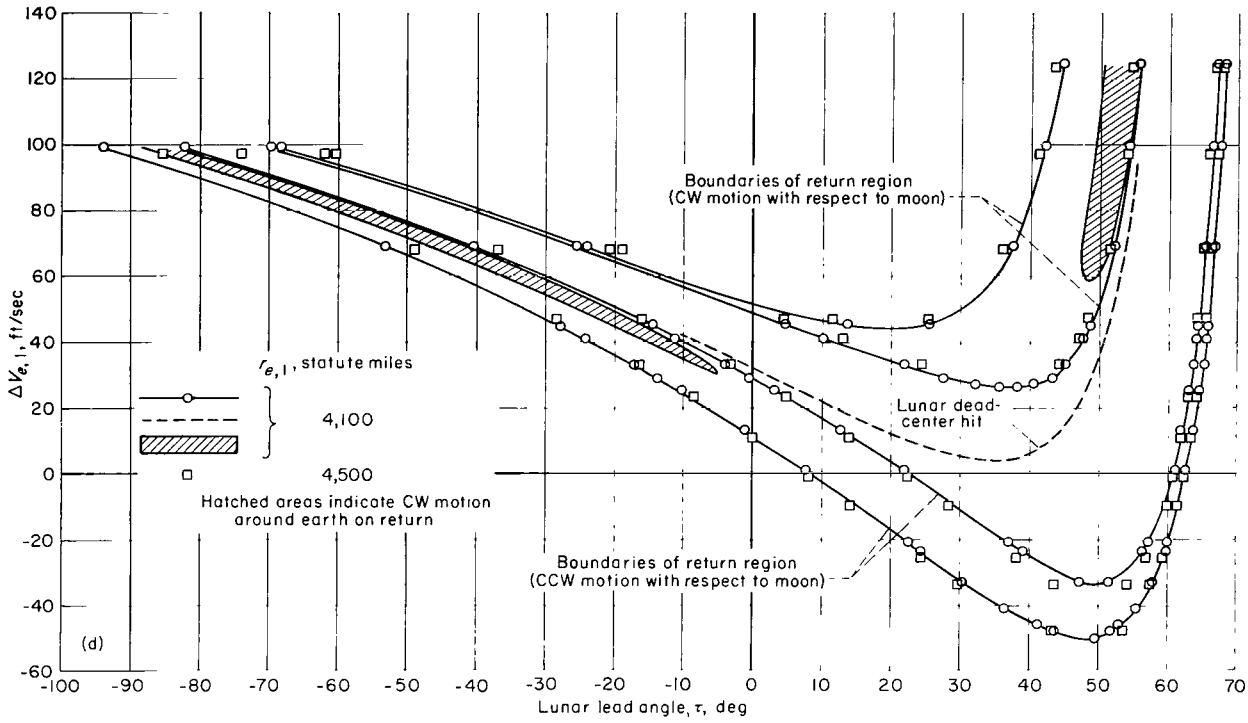

(d) $\gamma_{e,1}=40°$.

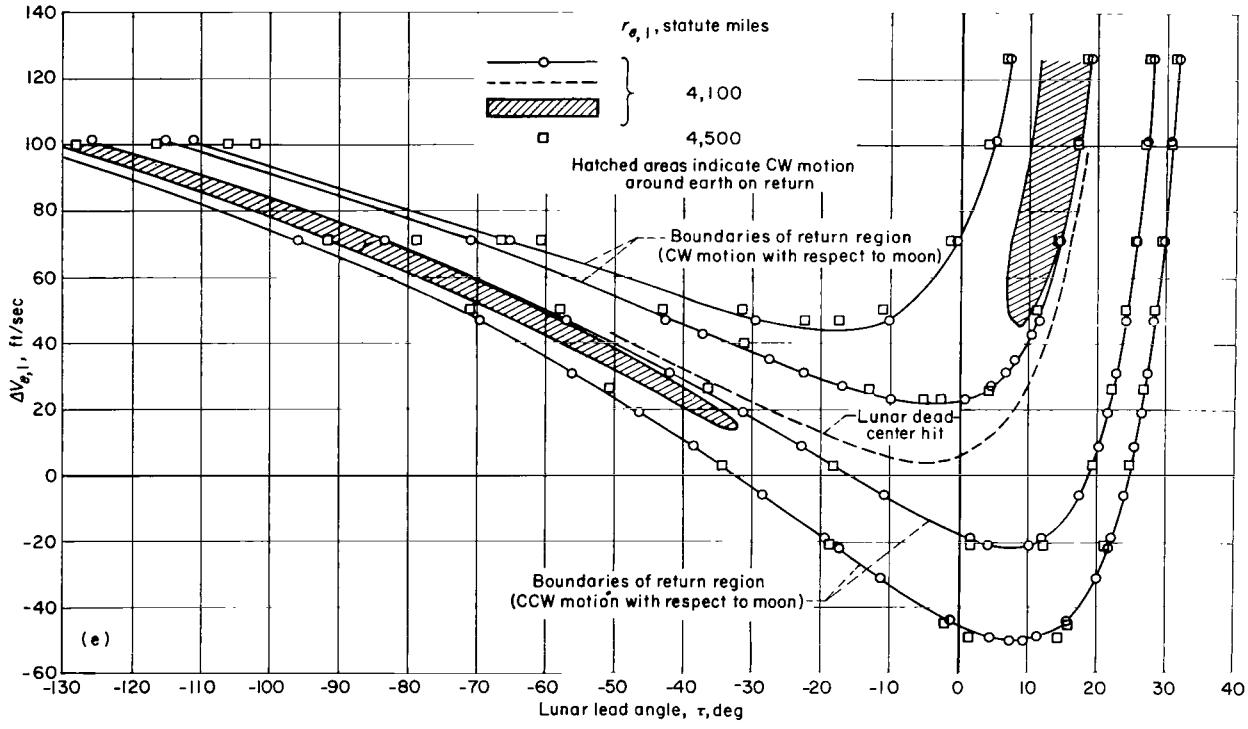

(e) $\gamma_{e,1}=60°$.

FIGURE 12.—Concluded.

Overall examination of figures 12(a) to 12(e) shows that as the value of the insertion flight-path angle is increased, a greater range of lead angle which will provide a return to the earth within the specified altitude of 40 miles is available at any given value of $\Delta V_{e,1}$.

The results of figure 12 can be superimposed on those of figure 4 to show possible insertion conditions which result in a trajectory that will miss the center of the moon by a specified distance and return to within an altitude of 40 statute miles. An example of such a superposition is shown in figure 13 for an insertion radius of 4,100 statute miles and a flight-path angle of 40°. The hatched regions represent the insertion conditions which produce trajectories that return the vehicle to within an altitude of 40 statute miles. The upper hatched region represents circumlunar trajectories while the lower hatched region yields trajectories that do not encompass the moon.

Total trip times for return to earth. —For lunar missions intended for a ballistic return of the vehicle to the vicinity of the earth, the total trip time required is an important variable. In figure 14 the total trip time from insertion to return is shown as a function of lunar miss distance. The data are shown for a range of incremental insertion velocities as well as for two insertion radii and two insertion flight-path angles.

The data in figure 14(a) correspond to ballistic trajectories in which the vehicle motion inside the lunar sphere of influence is clockwise with respect to the moon. In figure 14(b) the vehicle motion is counterclockwise. As indicated in the figure, each curve is considered to be composed of an upper branch and a lower branch. In figure 14(a) the trip times represented by the lower branch correspond to trajectories in which perilune is reached while the vehicle is moving away from the earth (part A of fig. 5); the upper branch corresponds to part B of figure 5. In figure 14(b), these designations are reversed.

Also indicated in the figure is the return perigee altitude. Dashed lines represent trajectories in which the return perigee altitude is greater than 40 statute miles; solid lines represent trajectories in

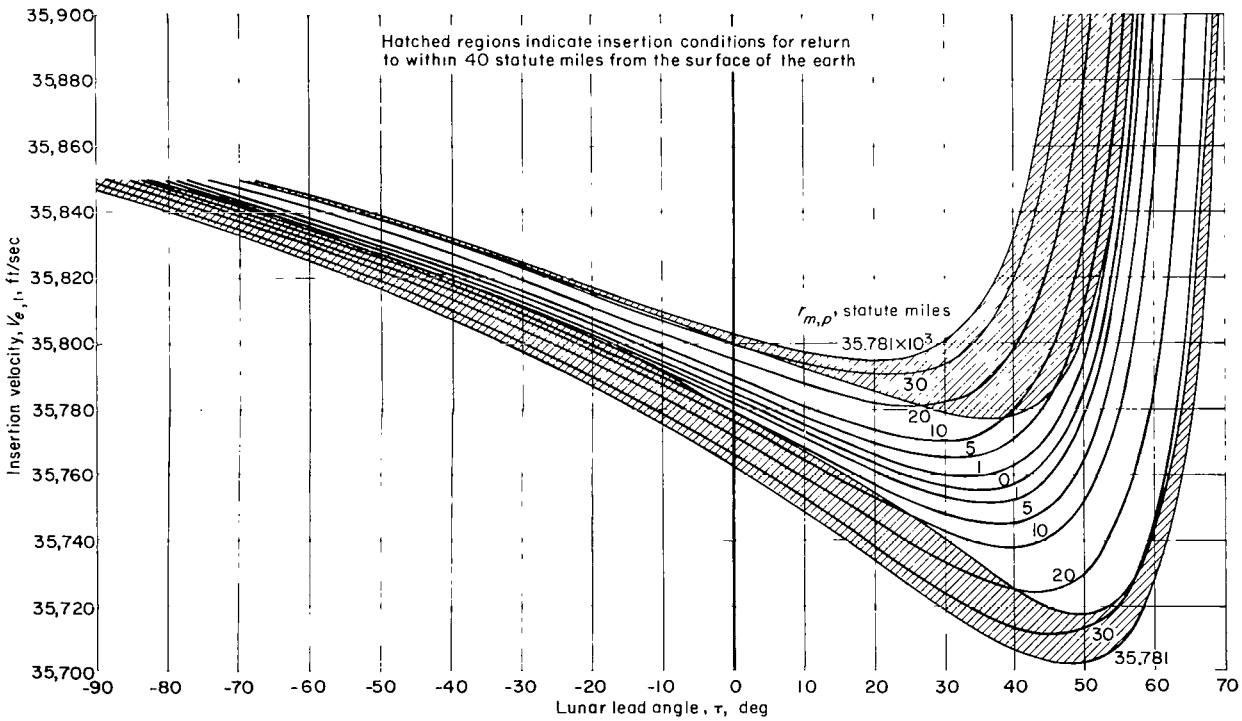

FIGURE 13.—Example of possible combinations of insertion velocity and lunar lead angle required for a given lunar miss distance and a return to within 40 statute miles from the surface of the earth. Insertion radius $r_{e,1}=4{,}100$ statute miles, insertion flight-path angle $\gamma_{e,1}=40°$.

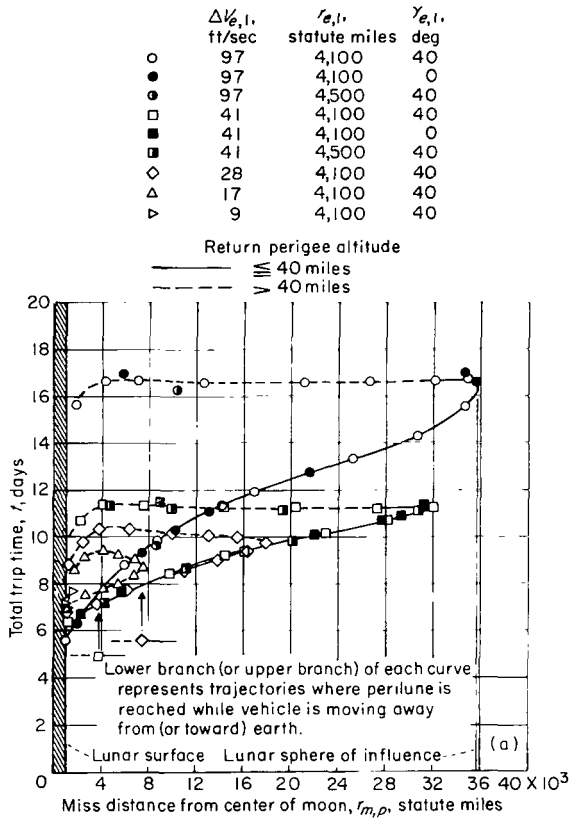
$\Delta V_{e,1}$, ft/sec
$r_{e,1}$, statute miles
$\gamma_{e,1}$, deg
97 4,100 40
97 4,100 0
97 4,500 40
41 4,100 40
41 4,100 0
41 4,500 40
28 4,100 40
17 4,100 40
9 4,100 40
Return perigee altitude
≦ 40 miles
> 40 miles
Total trip time, t, days
Lower branch (or upper branch) of each curve represents trajectories where perilune is reached while vehicle is moving away from (or toward) earth.
Lunar surface
Lunar sphere of influence
(a)
Miss distance from center of moon, $r_{m,p}$, statute miles

(a) Clockwise motion with respect to moon.

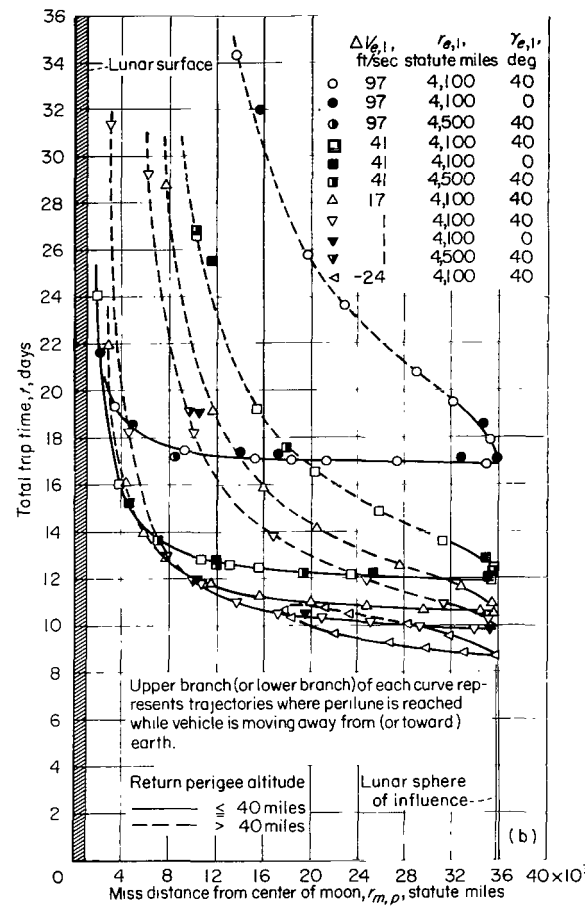
Lunar surface
$\Delta V_{e,1}$, ft/sec
$r_{e,1}$, statute miles
$\gamma_{e,1}$, deg
97 4,100 40
97 4,100 0
97 4,500 40
41 4,100 40
41 4,100 0
41 4,500 40
17 4,100 40
1 4,100 40
1 4,100 0
1 4,500 40
-24 4,100 40
Total trip time, t, days
Upper branch (or lower branch) of each curve represents trajectories where perilune is reached while vehicle is moving away from (or toward) earth.
Return perigee altitude
≦ 40 miles
> 40 miles
Lunar sphere of influence
(b)
Miss distance from center of moon, $r_{m,p}$, statute miles

(b) Counterclockwise motion with respect to moon.

FIGURE 14.—Total trip time from insertion to return.

which the return perigee altitude is 40 statute miles or less. This delineation, shown for $\gamma_{e,1}=40°$ and $r_{e,1}=4{,}100$ miles at the given values of $\Delta V_{e,1}$, was determined from figure 13. The delineation is not affected by insertion radius but differs for other values of $\gamma_{e,1}$. (See previous discussion of fig. 12.)

The results given in figure 14 can be used to obtain, to a good estimation, the total trip time required for any lunar ballistic mission. Interpolation may be employed to determine trip times for any given incremental insertion velocity. Overall inspection of the figure indicates that the effect of insertion radius on total trip time is relatively small. Also, the effect of flight-path angle is small except at the longer trip times for cases in which perilune is reached while the vehicle is moving away from the earth. (See upper branches of the curves in fig. 14(b).)

For the ballistic trajectories represented in figure 14(b) it is seen that for a near miss of the lunar surface, the total trip time would be exceptionally long. It is apparent from figure 14(a) that the most practical trajectories in regard to total trip time are those in which the vehicle rotates clockwise with respect to the moon. As previously noted, this type of trajectory would revolve around the far side of the moon. It may be noted in figure 14(a), however, that a very close miss of the lunar surface with return to within an altitude of 40 statute miles is attained only for the highest incremental insertion velocity shown ($\Delta V_{e,1}=97$ ft/sec).

EFFECTS OF ASSUMED LUNAR ORBIT

The data thus far presented in the charts are based on the assumptions given earlier in the paper. Three of these assumptions—the orbit of the moon is circular, the moon is at an average distance from the earth, and the moon is rotating

about the earth at an average velocity—have an important effect on the data presented herein. Insertion conditions selected from these charts will not result in the desired trajectory when the moon's position in its actual orbit does not correspond to that in the assumed average orbit. Assumed circular orbits with radii corresponding to the moon at apogee, perigee, and average distances from the earth are compared with the actual orbit of the moon in figure 15.

Errors caused by assumed lunar orbit.—In order to make an estimate of the error due to assuming an average orbit, data for a number of cases were computed with the moon at the extremes of its orbit.[1] These computations were made by using insertion conditions for dead-center hits obtained from figure 4 and from figure 1. The results of these calculations are shown in figure 16 as the variation of lunar miss distance (from center of moon) with trip time to perilune. Because the cases chosen resulted in dead-center hits for the moon at the average distance, the miss distances shown represent errors in miss distance due to using insertion conditions based on average values for calculating trajectories with the moon near apogee or perigee. (The miss-distance errors given in fig. 16 apply only to two-body two-dimensional calculations.) It is seen from the data of figure 16 that for trip times less than about 4 days the error can be only as much as about 4,000 statute miles, while for longer trip times the error can become greater than the radius of the lunar sphere of influence (35,781 statute miles). The smaller errors ($<$4,000 statute miles) occur for trajectories which arrive at or near the moon while the vehicle is moving away from the earth.

Insertion-condition corrections for true lunar orbit.—The previously mentioned errors in miss distance can be accounted for by changing the lead angle and/or the insertion velocity. The magnitude of the change required in lead angle and/or insertion velocity to achieve a given mission with the moon near apogee or perigee can be determined from the curves given in figure 17. The curves represent the lunar impact boundaries

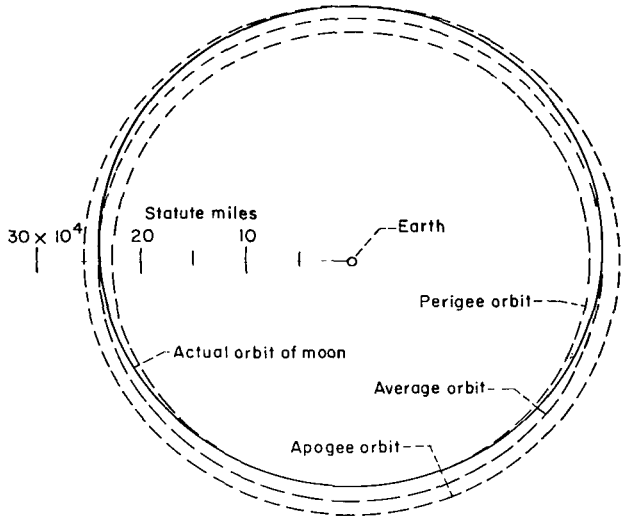

FIGURE 15.—Comparison of assumed circular lunar orbits with actual elliptical lunar orbit.

for three configurations of the earth-moon model: the moon rotating about the earth in a circular orbit with a radius equal to its nearest (perigee), average, or farthest (apogee) distance from the earth. The $\Delta V_{e,1}$ values used for plotting the data of each configuration apply to the $(V_{e,1})_{min}$ values for the moon at average distance as obtained from figure 2. The data in figure 17 are shown for insertion flight-path angles of 10° and 40°. The lines form the boundaries for an insertion radius of 4,100 statute miles whereas the symbols represent data for a radius of 4,500 statute miles. The dashed lines are for the average orbit (taken from fig. 1) and the solid lines for the apogee and perigee lunar orbits.

It is seen from the data of figures 17(a) and 17(b) that for a given lead angle (or insertion velocity) the change in the value of insertion velocity (or lead angle) from that required for the moon at an average distance from the earth is essentially independent of insertion flight-path angle and insertion radius. The maximum change in velocity is about 20 ft/sec whereas the maximum change in lead angle is about 20° (1⅓ hours change in launch time). These maximum changes apply to trajectories which require long trip times to perilune.

An interesting observation from figure 17 is that for trajectories which impact on the moon while the vehicle is moving away from the earth

[1] For these cases, all constants in English units, except D and ω_m, are the same as those given in table II. The values of ω_m taken for the perigee orbit and the apogee orbit were 0.00017073639 deg/sec and 0.00013704371 deg/sec, respectively. Also, D (1 lunar unit) for the perigee orbit was taken as 225,744 statute miles and for the apogee orbit, as 251,970 statute miles; therefore, all constants in lunar units change accordingly.

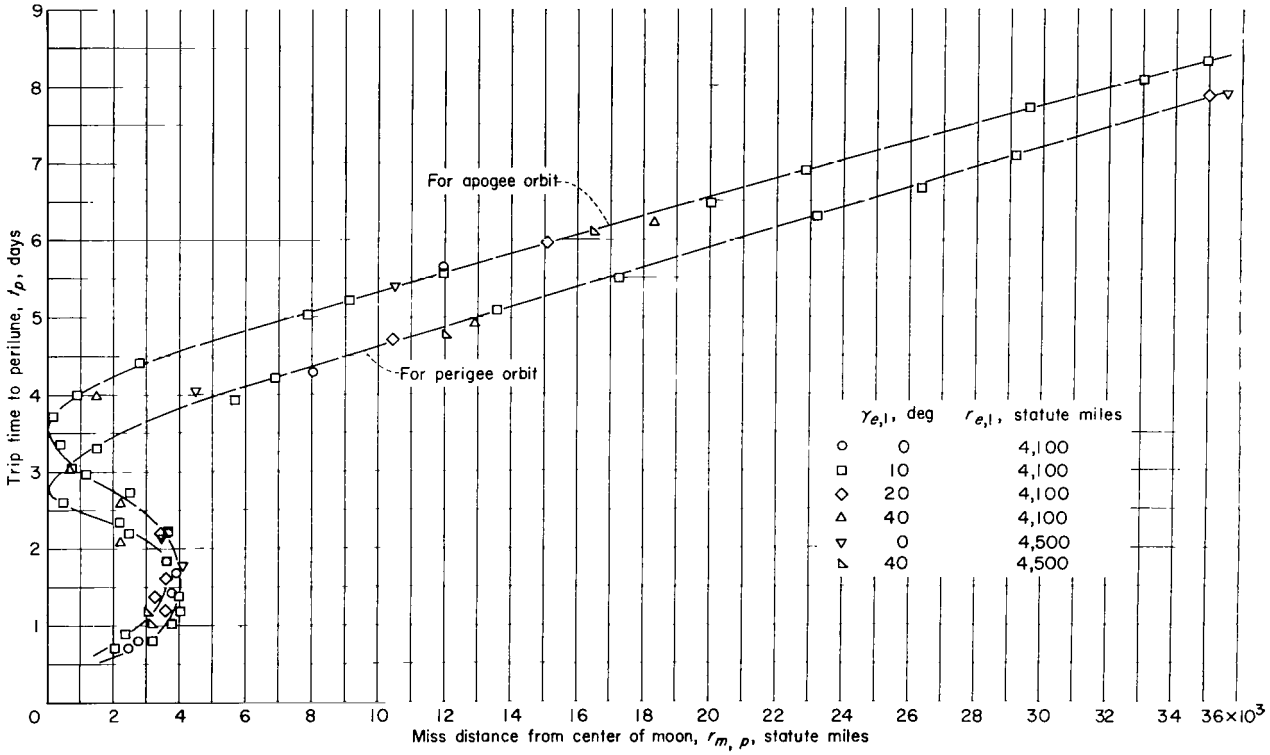
Trip time to perilune, t_p, days
Miss distance from center of moon, $r_{m,p}$, statute miles
For apogee orbit
For perigee orbit
$\gamma_{e,I}$, deg
$r_{e,I}$, statute miles
0 4,100
10 4,100
20 4,100
40 4,100
0 4,500
40 4,500
0 2 4 6 8 10 12 14 16 18 20 22 24 26 28 30 32 34 36×10³
0 1 2 3 4 5 6 7 8 9

FIGURE 16.—Lunar miss distance error for two assumed circular lunar orbits using initial conditions resulting in dead-center hits for an average circular lunar orbit.

(portion of curves to right of minimum velocity to impact) the lead angle required for a lunar impact is insensitive to the distance between the earth and the moon for an incremental insertion velocity of about 55 ft/sec.

Information obtained from figure 17 may be applied to any of the previous charts to correct the velocity and/or lead angle for missions when the moon is not near its average distance from the earth. The curves can be used directly when the moon is at its maximum or minimum distance from the earth and linear interpolation between the curves will be adequate for cases when the moon is at any other particular distance.

VALIDATION OF RESULTS

In order to obtain an insight into the applicability of the results obtained by the method of this report, comparisons were made by using results obtained from the classic restricted three-body equations of motion. Comparisons were made for 20 cases and are summarized in table III. The perilune radius (miss distance from the center of the moon) was used as a basis of comparison; that is, the perilune radius was calculated by the two methods for each set of tabulated insertion conditions. The insertion conditions for the first six cases were obtained from reference 3, and the results for the three-body method were obtained by both a two-dimensional and a three-dimensional analysis. Three-body results for the other cases are shown for a two-dimensional analysis. Insertion conditions for case 7 were obtained from reference 4, and insertion conditions for the remaining cases were selected from data pertaining to the present calculations made with the two-body equations. Calculations with the three-body equations were made, as in the case of the two-body equations, with the assumptions that the earth and moon are point masses, the lunar orbit is circular, and the effects of all other perturbing bodies are negligible. In contrast to the two-body equations used, the moon in the classic three-body equations is considered to rotate about the center of mass of the earth and moon.

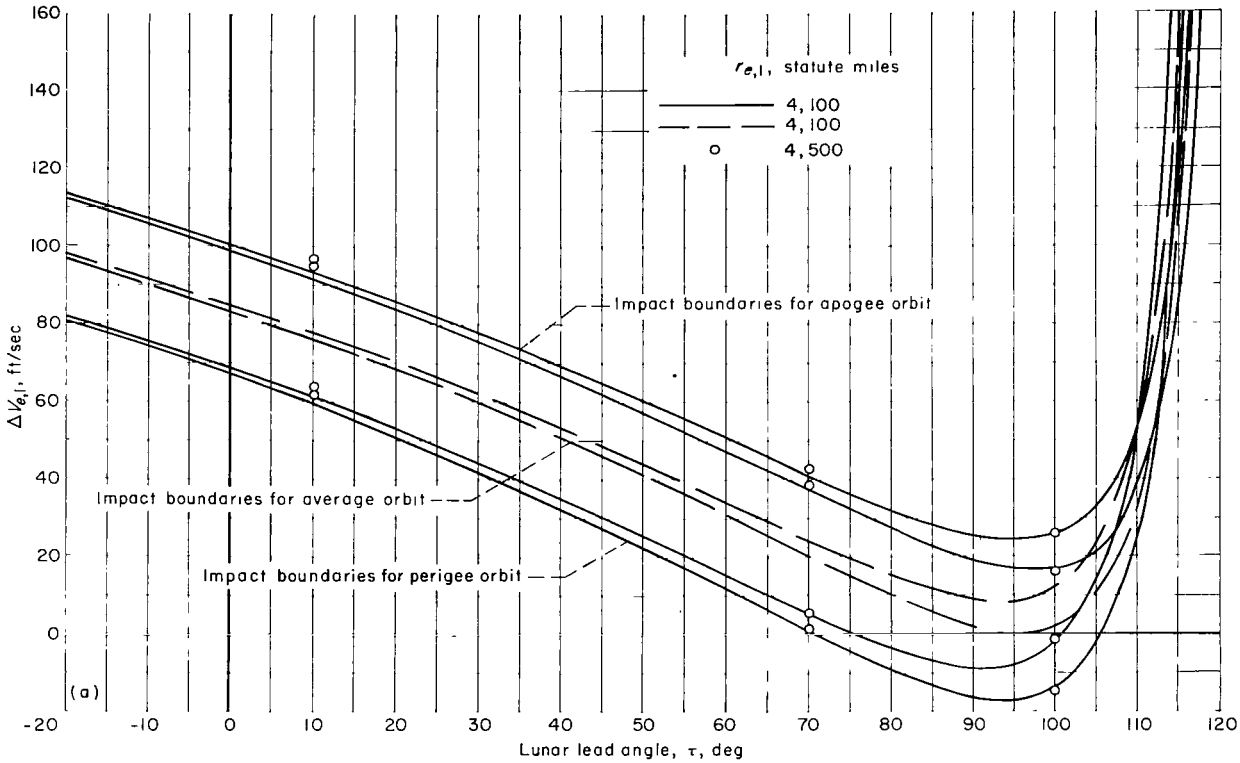

(a) $\gamma_{e,1}=10°$.

FIGURE 17.—Comparison of insertion velocity and lunar lead angle required for lunar impact for three assumed circular lunar orbits.

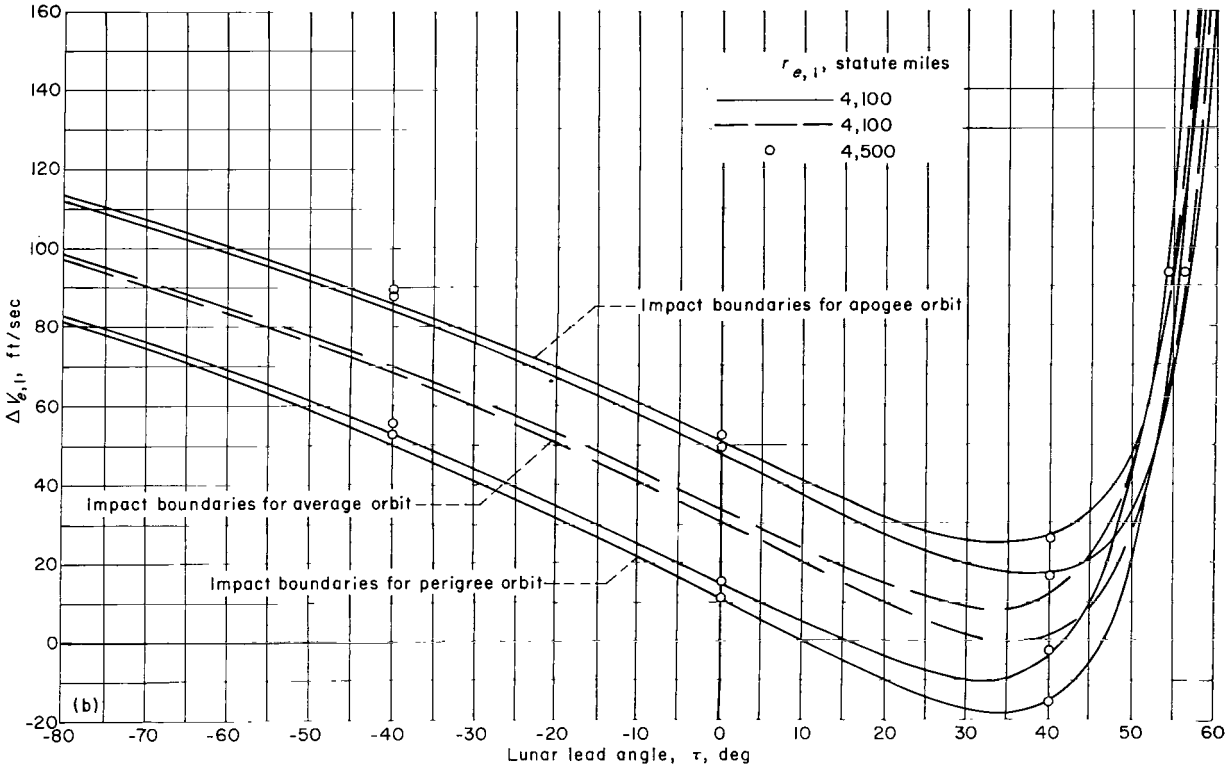

(b) $\gamma_{e,1}=40°$.

FIGURE 17.—Concluded.

TABLE II.—CONSTANTS FOR AVERAGE EARTH-TO-MOON DISTANCE

	English units	Lunar units
Distance between center of earth and center of moon, D	1,261,164,960 ft or 238,857 statute miles	1 lunar unit
Radius of moon, R_m	5,702,400 ft or 1,080 statute miles	0.0045215 lunar unit
Rotational velocity of moon about center of earth, ω_m	0.00015250415 deg/sec or 0.0000026616995 radian/sec	13.17635854 deg/day or 0.22997084 radian/day
Product of universal gravitational constant and mass of earth, μ_e	1.4077×10^{16} ft^3/sec^2	0.052386804 (lunar units)^3/day^2
Product of universal gravitational constant and mass of moon, μ_m	1.7282996×10^{14} ft^3/sec^2	0.0006431775 (lunar units)^3/day^2
Radius of sphere of influence of moon, r_m*	188,923,680 ft or 35,781 statute miles	0.1498 lunar unit

TABLE III.—COMPARISON OF RESULTS FROM PRESENT METHOD AND THREE-BODY METHOD

Case	Insertion conditions				Perilune or miss distance, statute miles, for—		
	$V_{e,1}$, ft/sec	$r_{e,1}$, statute miles	$\gamma_{e,1}$, deg	τ, deg	Present 2-body method (two-dimensional)	3-body method (two-dimensional)	3-body method (three-dimensional)
1	35, 101	4, 259	24. 00	81. 10	73	174	0
2	35, 242	4, 259	21. 02	95. 00	1, 224	1, 380	0
3	35, 597	4, 259	17. 26	104. 30	2, 194	2, 380	0
4	35, 101	4, 259	24. 00	81. 76	573	780	0
5	35, 242	4, 259	21. 02	95. 66	3, 214	3, 360	0
6	35, 597	4, 259	17. 26	104. 95	4, 688	4, 850	0
7	34, 950	4, 300	22	90	5, 467	4, 080	--------
8	35, 727	4, 100	10	90	30, 060	28, 200	--------
9	35, 735	4, 100	10	90	20, 764	20, 100	--------
10	35, 745	4, 100	10	90	9, 659	10, 100	--------
11	35, 749. 5	4, 100	10	90	5, 143	6, 500	--------
12	35, 755	4, 100	10	90	523	1, 680	--------
13	35, 758	4, 100	10	90	10	215	--------
14	35, 761. 8	4, 100	10	90	964	455	--------
15	35, 767	4, 100	10	90	4, 804	3, 630	--------
16	35, 773	4, 100	10	90	10, 124	8, 300	--------
17	35, 784	4, 100	10	90	20, 627	17, 150	--------
18	35, 797	4, 100	10	90	30, 994	26, 750	--------
19	35, 500	4, 159	0	114. 57	1	49	--------
20	35, 000	4, 300	0	132. 31	2, 350	2, 034	--------

The comparisons in table III show that roughly the same miss distances are obtained by both methods using two-dimensional analysis. In general, for perilune radii less than 2,000 statute miles, differences between the two methods were only several hundred miles. For perilune radii near 35,781 statute miles (the radius of the lunar sphere of influence), the maximum difference was only about 4,000 miles. The three-body three-dimensional results (first six cases) also show reasonable agreement with the present results. For the three-dimensional analysis, the initial angle between the vehicle trajectory plane and earth-moon plane was either 16° or 18.4° (ref. 3). Three-dimensional calculations using a much larger angle would probably indicate a greater difference from the present two-body two-dimensional calculations. Based on the comparisons in table III, it is concluded that the insertion conditions given herein can be considered good approximations to those needed to calculate trajectories for lunar missions with more detailed models of the earth-moon system.

CONCLUDING REMARKS

A study of insertion requirements for two-dimensional lunar ballistic trajectories has been made with the use of simple two-body equations of motion. Comparisons with two-dimensional and three-dimensional results obtained with the more complete three-body equations of motion indicated that the data presented herein are a very good first approximation to the results obtained from the more sophisticated equations. It appears, therefore, that the insertion conditions presented herein are adequate for the preliminary calculation of any desired trajectory with more sophisticated equations of motion.

The main objective of the study was to provide summary charts for use in selecting approximate insertion conditions (velocity, distance from center of earth, flight-path angle, and lunar lead angle or firing time) required for lunar missions intended to come within the lunar sphere of influence (radius of 35,781 statute miles). Where convenient, the results were normalized by basing the insertion velocity on the minimum insertion velocity required for lunar impact for a particular insertion radius and insertion flight-path angle. By normalizing the results in this manner it was shown that trip time to perilune (closest approach to moon) as well as total trip time to return to earth are essentially independent of insertion radius and insertion flight-path angle. Also shown to be practically independent of these two insertion conditions were the lunar longitude limits for impacts on the moon, lunar longitude of perilune, and the vehicle velocity at perilune. In addition, for given values of insertion flight-path angle, normalized plots of insertion velocity and lunar lead angle required to return to within a specified distance of the earth showed the data to be generally independent of insertion radius.

The insertion requirements given in the summary charts pertain to calculations made for an assumed circular lunar orbit with a radius equal to the average distance between the moon and the earth. Data have been included, however, to permit use of the charts for determining insertion requirements when the moon is at either extreme in its actual orbit. For trajectories resulting in relatively short trip times to perilune (<4 days) the maximum miss-distance error due to use of insertion conditions based on an average earth-to-moon distance was found to be only about 4,000 miles, whereas for longer trip times the error could become greater than the radius of the lunar sphere of influence. For the moon at either extreme of its orbit the maximum difference in insertion velocity from that based on an average circular lunar orbit was shown to be about 20 ft/sec. The maximum difference in lunar lead angle was about 20° (1⅓ hours change in launch time). Also, these differences were shown to be essentially independent of the insertion flight-path angle and/or insertion radius.

LANGLEY RESEARCH CENTER,
NATIONAL AERONAUTICS AND SPACE ADMINISTRATION,
LANGLEY AIR FORCE BASE, VA., *August 10, 1961.*

APPENDIX A

SYMBOLS

The English system of units is used in this study. In case conversion to metric units is desired, the following relationships apply: 1 foot=0.3048 meter, and 1 statute mile = 5,280 feet = 1,609.3 meters.

The quantities given in this list of symbols are defined graphically in figures 18 to 22.

A	angle between geocentric vehicle velocity vector and selenocentric vehicle velocity vector at entry into or exit from lunar sphere of influence, deg
B	angle between geocentric and selenocentric radius vector at entry into or exit from lunar sphere of influence, deg
C	angle between geocentric vehicle velocity vector and tangential orbital velocity vector of moon at entry into or exit from lunar sphere of influence, deg
D	distance between center of earth and center of moon, ft or statute miles
E	eccentric anomaly, radians
F	auxiliary quantity corresponding to the eccentric anomaly in elliptic orbits, radians
K	angle between line joining centers of earth and moon and selenocentric radius vector at entry into or exit from lunar sphere of influence, deg
L	lunar longitude, measured clockwise in the plane of motion (looking down on north pole of moon), deg
M	moon
p	semilatus rectum of orbit, ft
R_m	radius of moon, ft or statute miles
r	radial distance of vehicle from center of earth or moon, ft or statute miles
r_e*	radius of sphere of influence of earth, ft or statute miles
r_m*	radius of sphere of influence of moon, ft or statute miles
t	trip time, sec or days
Δt	incremental trip time, sec
V	vehicle inertial velocity, ft/sec
$(V_{e,1})_{min}$	minimum insertion velocity for lunar impact for given insertion radius and insertion flight-path angle, ft/sec
$\Delta V_{e,1}$	incremental insertion velocity, $V_{e,1} - (V_{e,1})_{min}$, ft/sec
$(V_{e,1})_H$	insertion velocity required for lunar dead-center hit for given insertion radius, insertion flight-path angle, and lunar lead angle, ft/sec
V_ω	tangential velocity of moon in assumed circular orbit, ft/sec
X_e, Y_e	inertial rectangular coordinate axes with origin at center of earth
X_m, Y_m	inertial rectangular coordinate axes with origin at center of moon
2	point of entry into lunar sphere of influence
3	point of exit from lunar sphere of influence
α	angle between radius vector and velocity vector, deg
Γ	angle through which velocity vector is rotated within lunar sphere of influence, deg
γ	flight-path angle; angle between velocity vector and line perpendicular to radius vector, deg
ϵ	eccentricity
η	angle between geocentric radius vector and line joining centers of earth and moon, deg
θ	angle measured from perigee (or perilune) radius vector to vehicle radius vector from center of earth (or moon), deg

$\theta_{e,x}$ angle measured from X_e-axis to geocentric radius vector, deg

$\theta_{m,x}$ angle measured from X_m-axis to selenocentric radius vector, deg

θ_0 angle measured from perilune radius vector to X_m-axis, deg

Λ angle between perilune radius vector and selenocentric velocity vector at exit from lunar sphere of influence, deg

λ orientation angle of major axis of earth departure trajectory with respect to line joining centers of earth and moon at insertion, deg

$\Delta\lambda$ angular difference between major axes of earth departure and return orbits, deg

μ_e product of universal gravitational constant and mass of earth, ft^3/sec^2

μ_m product of universal gravitational constant and mass of moon, ft^3/sec^2

τ lunar lead angle; angle between geocentric radius vector and line joining centers of earth and moon at insertion, $180-(\lambda+\theta_{e,1})$, deg

τ_H lunar lead angle required for lunar dead-center hit for given insertion radius, insertion flight-path angle, and insertion velocity, deg

ϕ angle measured from X_m-axis to selenocentric radius vector at entry into lunar sphere of influence, deg

ψ angle measured from X_m-axis to selenocentric velocity vector at exit from lunar sphere of influence, deg

ω_m rotational velocity of moon about center of earth, deg/sec or radians/sec

Subscripts:

1 value at insertion

2 value at entry into lunar sphere of influence

3 value at exit from lunar sphere of influence

e referred to earth coordinate system

I referred to value at lunar impact

m referred to moon coordinate system

p perigee or perilune

s circular satellite velocity

t any given time

A prime denotes that a value is measured from the perigee radius vector of the return trajectory. The absolute value of any term is denoted by $|\ |$.

APPENDIX B

EQUATIONS OF MOTION

The basic assumptions used in this study have been discussed in the main body of the paper. Therefore, only the equations of motion are presented in this section. In addition to the specific equations needed to obtain the results of this paper, general equations needed for a detailed analysis of the trajectory to and from the moon are given. Figures 18 to 22 are presented to show positive directions for angles and to aid in visualizing the equations.

Because of the magnitude of the equation constants in English units, it was convenient to perform the calculations in lunar units. In addition, time was taken in terms of days. The computed results were then converted to English units. The constants are given in table II in both English and lunar units for the moon at an average distance from the earth.

The first group of equations ((B1) to (B11)) is used to compute the earth departure trajectory. As mentioned previously, this trajectory can be either elliptic, parabolic, or hyperbolic. The equations are as follows:

For computing the distance from the center of the earth for any given value of θ_e,

$$r_e=\frac{p_{e,1}}{1+\epsilon_{e,1}\cos\theta_e} \tag{B1}$$

where θ_e is measured counterclockwise from the perigee radius vector to the vehicle radius vector of the point in question. The semilatus rectum of the departure trajectory is

$$p_{e,1}=r_{e,1}\left[\frac{V_{e,1}}{(V_{e,s})_1}\right]^2\cos^2\gamma_{e,1} \tag{B2}$$

where $r_{e,1}$ is the insertion radius vector from the center of the earth, $V_{e,1}$ is the insertion inertial velocity, $\gamma_{e,1}$ is the insertion inertial flight-path angle measured with respect to the local spherical horizontal, and circular satellite velocity at $r_{e,1}$ is

$$(V_{e,s})_1=\sqrt{\frac{\mu_e}{r_{e,1}}} \tag{B3}$$

The eccentricity of the earth departure trajectory is

$$\epsilon_{e,1}=\frac{1}{\cos\theta_{e,1}}\left(\frac{p_{e,1}}{r_{e,1}}-1\right) \tag{B4}$$

where

$$\tan\theta_{e,1}=\tan\gamma_{e,1}\left[\frac{p_{e,1}/r_{e,1}}{(p_{e,1}/r_{e,1})-1}\right] \tag{B5}$$

For computing the inertial velocity at any point in the earth departure trajectory,

$$V_e=\sqrt{\mu_e\left(\frac{2}{r_e}-\frac{1-\epsilon_{e,1}^2}{p_{e,1}}\right)} \tag{B6}$$

For computing the inertial flight-path angle at any point,

$$\tan\gamma_e=\frac{\epsilon_{e,1}\sin\theta_e}{1+\epsilon_{e,1}\cos\theta_e} \tag{B7}$$

For computing the time from insertion to any point,

$$t=t(\theta_e)-t(\theta_{e,1}) \tag{B8}$$

where $t(\theta_e)$ is time from perigee to the point in question and $t(\theta_{e,1})$ is the time from perigee to insertion. The value of $t(\theta_e)$ is computed as follows:

If $\epsilon_{e,1}<1$ (elliptic trajectory),

$$t(\theta_e)=\frac{p_{e,1}}{1-\epsilon_{e,1}^2}\sqrt{\frac{p_{e,1}}{\mu_e}}\frac{1}{\sqrt{1-\epsilon_{e,1}^2}}(E-\epsilon_{e,1}\sin E) \tag{B9}$$

where E is the eccentric anomaly and

$$\tan\frac{E}{2}=\sqrt{\frac{1-\epsilon_{e,1}}{1+\epsilon_{e,1}}}\tan\frac{\theta_e}{2} \tag{B9a}$$

If $\epsilon_{e,1}>1$ (hyperbolic trajectory),

$$t(\theta_e)=\frac{p_{e,1}}{{\epsilon_{e,1}}^2-1}\sqrt{\frac{p_{e,1}}{\mu_e}}\frac{1}{\sqrt{{\epsilon_{e,1}}^2-1}}(-F+\epsilon_{e,1}\sinh F) \tag{B10}$$

where F is an auxiliary quantity in hyperbolic orbits corresponding to the eccentric anomaly in elliptic orbits, and

$$\tanh\frac{F}{2}=\sqrt{\frac{\epsilon_{e,1}-1}{\epsilon_{e,1}+1}}\tan\frac{\theta_e}{2} \tag{B10a}$$

If $\epsilon_{e,1}=1$ (parabolic trajectory),

$$t(\theta_e)=p_{e,1}\sqrt{\frac{p_{e,1}}{\mu_e}}\left(\frac{1}{2}\tan\frac{\theta_e}{2}\right)\left(1+\frac{1}{3}\tan^2\frac{\theta_e}{2}\right) \tag{B11}$$

The value of $t(\theta_{e,1})$ is computed by using the appropriate equation (eqs. (B9), (B10), or (B11)) and by substituting $\theta_{e,1}$ for θ_e. It should be noted that if insertion is at perigee the value of $t(\theta_{e,1})$ will be zero. Also, the angles $E/2$ and $F/2$ in equations (B9a) and (B10a) should always be considered to be in the same quadrant as $\theta_e/2$. The distances and angles in equations (B1) to (B11) are shown graphically in figure 18.

The next step in the calculations is to determine the point of entry of the departure trajectory into the lunar sphere of influence. The method used in this study was an iteration process which compared the distance from the center of the moon at a given value of θ_e with the radius of the lunar sphere of influence and computed the value of θ_e necessary to make this difference zero. This value of θ_e was then taken as $\theta_{e,2}$. The equation used to calculate the distance from the center of the moon was

$${r_m}^2=D^2+{r_e}^2-2r_eD\cos\eta \tag{B12}$$

where r_m is the distance from the center of the moon to the point on the trajectory under consideration and η is the angle between the radius vector from the earth and the line joining the centers of the earth and moon. The angle η is computed from the following equation:

$$\eta=\theta_e+\lambda-\omega_m t-180 \tag{B13}$$

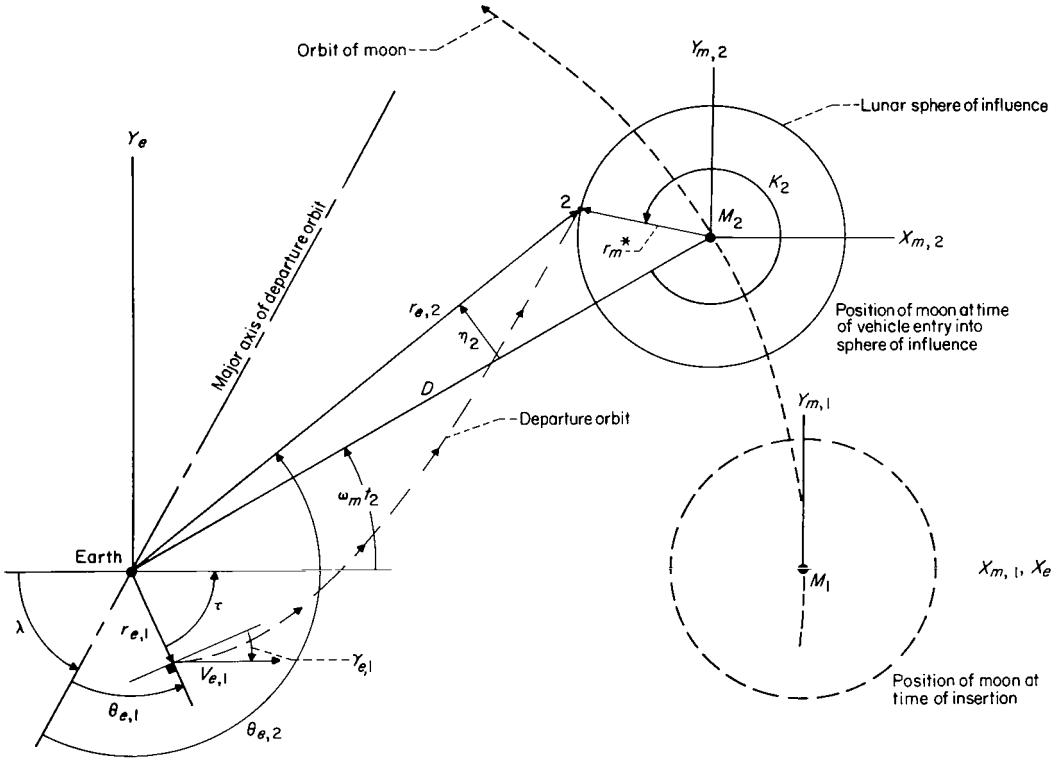

FIGURE 18.—Definition of parameters for earth departure orbit. Positive directions shown.

The angle λ is related to the lunar lead angle τ by the following equation:

$$\lambda=180-\theta_{e,1}-\tau \tag{B14}$$

where the lunar lead angle is the angle between the radius vector and a line joining the centers of the earth and moon at insertion. (See fig. 18.)

Once $\theta_{e,2}$ is obtained, then the geocentric values $r_{e,2}$, $V_{e,2}$, $\gamma_{e,2}$, and t_2 can be calculated for the point of entry. (See figs. 18 and 19.)

It should be noted that

$$\sin \eta_2 \leqq \frac{r_m^*}{D} \tag{B15}$$

and

$$(D-r_m^*) \leqq r_{e,2} \leqq (D+r_m^*) \tag{B16}$$

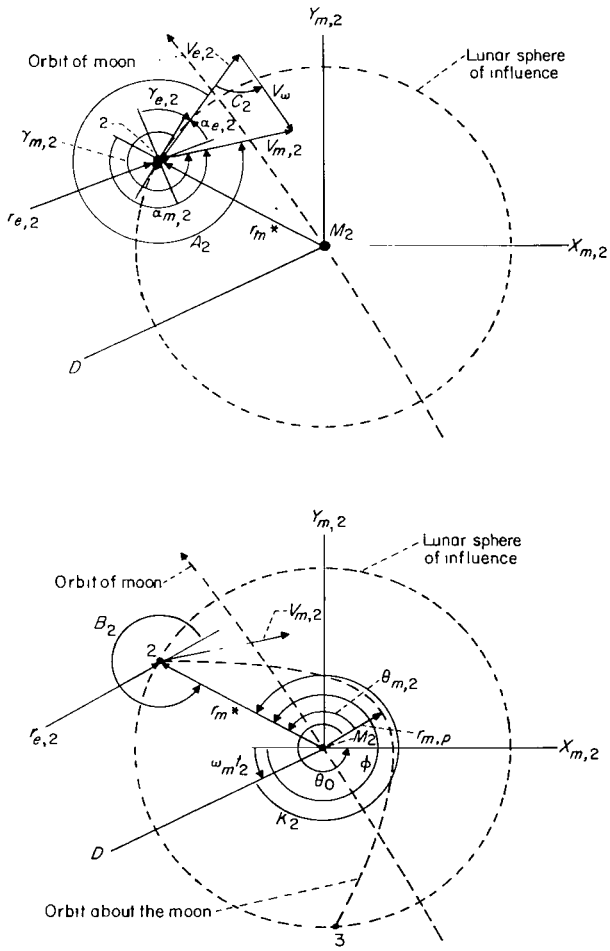

FIGURE 19.—Definition of parameters during vehicle entry into sphere of influence of the moon. Positive directions shown.

Equations (B17) to (B22) are used to convert velocity and flight-path angle at the point of entry to selenocentric values. The distance from the center of the moon $r_{m,2}$ is equal to r_m^*; the time is the same in the two coordinate systems. For converting velocity,

$$V_{m,2}^2=V_{e,2}^2+V_\omega^2-2V_{e,2}V_\omega \cos C_2 \tag{B17}$$

where the tangential velocity of the moon rotating about the earth is

$$V_\omega=D\omega_m \tag{B18}$$

and the angle C_2 is

$$C_2=90-\alpha_{e,2}-\eta_2=\gamma_{e,2}-\eta_2 \tag{B19}$$

The flight-path angle is converted by use of the following equation:

$$\gamma_{m,2}=-B_2+A_2-\gamma_{e,2} \tag{B20}$$

where

$$\sin B_2=\frac{-\sin \eta_2}{r_m^*/D} \tag{B21}$$

and

$$\sin A_2=-\frac{V_\omega}{V_{m,2}} \sin C_2 \tag{B22}$$

In order to have B_2 and A_2 in the proper quadrant, the following two rules may be used:

(1) The sign of cos B_2 is the sign of the quantity

$$D^2-r_{e,2}^2-(r_m^*)^2$$

(2) The sign of cos A_2 is the sign of the quantity

$$V_{e,2}^2+V_{m,2}^2-V_\omega^2$$

These angles and distances are shown in figure 19.

With all the trajectory parameters at point 2 converted to a selenocentric coordinate system, it is now possible to calculate the trajectory inside the sphere of influence of the moon. The following equations are used for this purpose:

For calculating the distance from the center of the moon for any given value of θ_m,

$$r_m=\frac{p_m}{1+\epsilon_m \cos \theta_m} \tag{B23}$$

where θ_m is the angle between the radius vector at perilune and the radius vector at the point in

question, and

$$p_m = r_m^* \left(\frac{V_{m,2}}{V_{m,s}}\right)^2 \cos^2 \gamma_{m,2} \tag{B24}$$

where the circular satellite velocity about the moon at r_m^* is

$$V_{m,s} = \sqrt{\frac{\mu_m}{r_m^*}} \tag{B25}$$

The eccentricity of the trajectory about the moon (always hyperbolic) is

$$\epsilon_m = \frac{1}{\cos \theta_{m,2}} \left(\frac{p_m}{r_m^*} - 1\right) \tag{B26}$$

where

$$\tan \theta_{m,2} = \tan \gamma_{m,2} \left[\frac{p_m/r_m^*}{(p_m/r_m^*) - 1}\right] \tag{B27}$$

The closest approach to the moon (perilune) occurs when θ_m is zero and, according to equation (B23), is

$$r_{m,p} = \frac{p_m}{1+\epsilon_m} \tag{B28}$$

For calculating velocity at any point,

$$V_m = \sqrt{\mu_m \left(\frac{2}{r_m} - \frac{1-\epsilon_m^2}{p_m}\right)} \tag{B29}$$

The velocity at perilune is

$$V_{m,p} = \sqrt{\mu_m \left(\frac{2}{r_{m,p}} - \frac{1-\epsilon_m^2}{p_m}\right)} \tag{B30}$$

For calculating the flight-path angle at any point,

$$\tan \gamma_m = \frac{\epsilon_m \sin \theta_m}{1+\epsilon_m \cos \theta_m} \tag{B31}$$

The calculation of the time interval inside the sphere of influence of the moon is sensitive to the direction of motion with respect to the moon (i.e., clockwise or counterclockwise). The direction of rotation with respect to the moon may be determined as follows:

The angle between the radius vector and the velocity vector is

$$\alpha_{m,2} = -90 + \gamma_{m,2} \tag{B32}$$

If $0° < \alpha_{m,2} < 180°$ the motion is counterclockwise or direct; if $180° < \alpha_{m,2} < 360°$ the motion is clockwise or retrograde. In practice, it is seen that $\gamma_{m,2}$ must always be in the third or fourth quadrant for a penetration of the lunar sphere of influence. Therefore, only values of $\alpha_{m,2}$ in the second or third quadrant need be considered. If $\alpha_{m,2}$ is 90° or 270°, the motion is tangential to the lunar sphere of influence, and if $\alpha_{m,2}$ is 180°, the motion is directly toward the center of the moon.

The time measured from perilune to any point on the trajectory about the moon is

$$t(\theta_m) = \sqrt{\frac{p_m}{\mu_m}} \left(\frac{p_m}{1-\epsilon_m^2}\right) \left[\frac{-\epsilon_m \sin \theta_m}{1+\epsilon_m \cos \theta_m} + \frac{1}{\sqrt{\epsilon_m^2 - 1}} \log_e \left(\frac{\epsilon_m + \cos \theta_m + \sin \theta_m \sqrt{\epsilon_m^2 - 1}}{1+\epsilon_m \cos \theta_m}\right)\right] \tag{B33}$$

For counterclockwise motion with respect to the moon the computed values of $t(\theta_m)$ will start negatively and increase positively. For clockwise motion $t(\theta_m)$ will start positively and decrease.

In order to compute the accumulated trip time from insertion, the following equation may be used:

$$t = t_2 + \frac{\sin \alpha_{m,2}}{|\sin \alpha_{m,2}|} [t(\theta_m) - t(\theta_{m,2})] \tag{B34}$$

where t_2 is the trip time up to the point of entering the lunar sphere of influence and the term $\frac{\sin \alpha_{m,2}}{|\sin \alpha_{m,2}|}$ is merely present to take into account the direction of motion with respect to the moon. The time $t(\theta_{m,2})$ is the time between entry into the lunar sphere of influence and perilune and is calculated from equation (B33) by substituting $\theta_{m,2}$ for θ_m. In determining the limits of θ_m for use in equation (B33) the following expression is useful:

$$\frac{\sin \alpha_{m,2}}{|\sin \alpha_{m,2}|} \theta_{m,2} \leqq \theta_m \leqq \frac{-\sin \alpha_{m,2}}{|\sin \alpha_{m,2}|} \theta_{m,2} \tag{B35}$$

For cases of lunar impact the following equations can be used to compute the conditions at impact:

For impact velocity,

$$V_I = \sqrt{\mu_m \left(\frac{2}{R_m} - \frac{1-\epsilon_m^2}{p_m}\right)} \tag{B36}$$

where R_m is the assumed radius of the moon.

For impact angle,

$$\tan \gamma_I = \frac{\epsilon_m \sin \theta_I}{1+\epsilon_m \cos \theta_I} \tag{B37}$$

where

$$\cos \theta_I = \frac{1}{\epsilon_m}\left(\frac{p_m}{R_m}-1\right) \tag{B38}$$

and the quadrant of θ_I can be determined from the following table:

Quadrant of $\theta_{m,2}$	Sign of $\cos \theta_I$	Quadrant of θ_I
1 or 2	+	1
1 or 2	−	2
3 or 4	−	3
3 or 4	+	4

For longitude of impact,

$$L_I = \theta_{m,2} - K_2 - \theta_I + \omega_m \Delta t_I \tag{B39}$$

where L_I is the longitude of impact measured in the plane of motion with 0° longitude defined by the intersection of the lunar surface with a line joining the centers of the earth and moon, and

$$K_2 = \eta_2 + B_2 \tag{B40}$$

as shown in figures 18 and 19. The term Δt_I is the incremental time between entry into the lunar sphere of influence and impact, and is

$$\Delta t_I = |t(\theta_{m,2}) - t(\theta_I)| \tag{B41}$$

where $t(\theta_I)$ is the time between the point of impact and perilune. The values of $t(\theta_{m,2})$ and $t(\theta_I)$ are obtained by substituting $\theta_{m,2}$ and θ_I for θ_m in equation (B33).

With the equations given up to this point, the trajectory up to and inside the lunar sphere of influence can be calculated in as much detail as is desired. In order to calculate the return trajectory, it is necessary first to calculate the selenocentric conditions at the point of exit from the lunar sphere of influence and then convert these conditions to geocentric conditions. The following relationships are used to calculate the selenocentric conditions at this point:

$$\theta_{m,3} = 360 - \theta_{m,2} \tag{B42}$$

$$r_{m,3} = r_m{}^* \tag{B43}$$

$$V_{m,3} = V_{m,2} \tag{B44}$$

$$\gamma_{m,3} = -\gamma_{m,2} \tag{B45}$$

$$K_3 = \psi - \omega_m t_3 - \alpha_{m,3} \tag{B46}$$

or since

$$\alpha_{m,3} = \gamma_{m,3} - 90 \tag{B47}$$

then

$$K_3 = \psi - \omega_m t_3 + 90 - \gamma_{m,3} \tag{B48}$$

where

$$\psi = \Lambda - \theta_0 \tag{B49}$$

and

$$\theta_0 = \theta_{m,2} - \phi + 180 \tag{B50}$$

Since

$$\phi = \omega_m t_2 + K_2 \tag{B51}$$

then

$$\theta_0 = -K_2 - \omega_m t_2 + \theta_{m,2} + 180 \tag{B52}$$

Also,

$$\Lambda = \gamma_{m,3} + \theta_{m,3} - 90 \tag{B53}$$

The total time from insertion to the point of exit from the sphere of influence of the moon is

$$t_3 = t_2 + 2|t(\theta_{m,2})| \tag{B54}$$

The longitude of perilune is

$$L_p = \left(\frac{\omega_m t_2 + \omega_m t_3}{2}\right) - \theta_0 + 180 \tag{B55}$$

As a matter of interest the angle through which the velocity vector is rotated within the lunar sphere of influence is

$$\Gamma = 180 + 2\Lambda \tag{B56}$$

The angles and distances in equations (B42) to (B56) are shown in figures 19 and 20.

To convert the selenocentric conditions at exit to geocentric conditions, equations (B57) to (B63) are used:

For converting distance from center of earth,

$$r_{e,3}{}^2 = (r_m{}^*)^2 + D^2 - 2r_m{}^* D \cos K_3 \tag{B57}$$

For converting velocity,

$$V_{e,3}{}^2 = V_{m,3}{}^2 + V_\omega{}^2 - 2V_{m,3}V_\omega \cos C_3 \tag{B58}$$

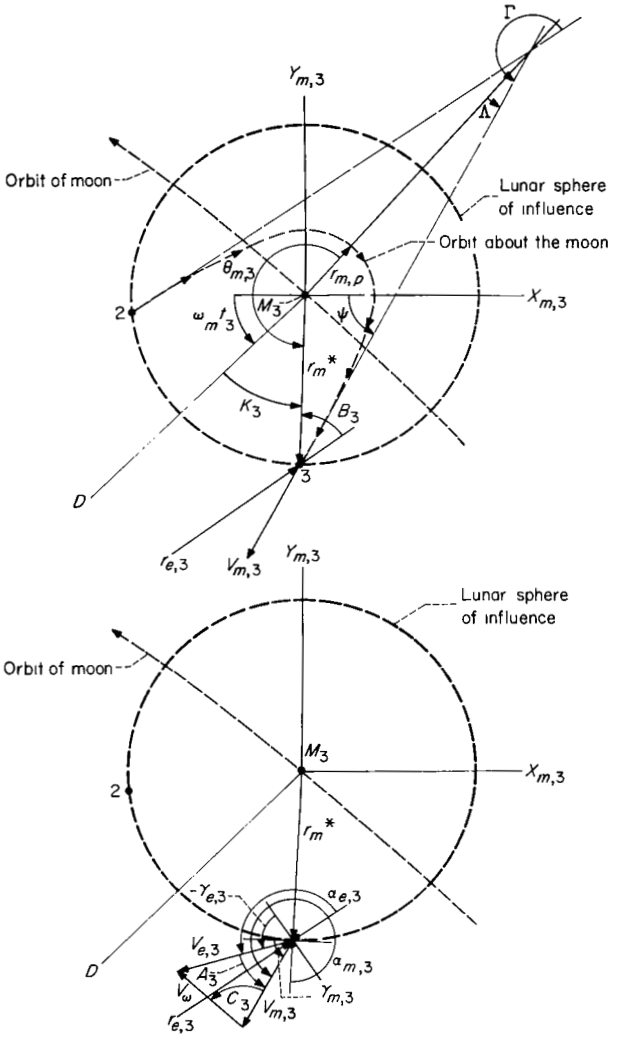

FIGURE 20.—Definition of parameters during vehicle exit from sphere of influence of the moon. Positive directions shown.

where

$$C_3=90-\psi+\omega_m t_3 \tag{B59}$$

For converting flight-path angle,

$$\gamma_{e,3}=A_3+C_3+\eta_3-180 \tag{B60}$$

where

$$\sin A_3=\frac{V_\omega}{V_{e,3}}\sin C_3 \tag{B61}$$

and the sign of cos A_3 is the same as the sign of the quantity ${V_{e,3}}^2+{V_{m,3}}^2-{V_\omega}^2$, and

$$\sin \eta_3=\frac{-{r_m}^*}{r_{e,3}}\sin K_3 \tag{B62}$$

where cos η_3 is always positive.

The direction of motion of the return trajectory about the earth is determined by solving for $\alpha_{e,3}$ as follows:

$$\alpha_{e,3}=90-\gamma_{e,3} \tag{B63}$$

If $0°<\alpha_{e,3}<180°$ the motion is counterclockwise about the earth, and if $180°<\alpha_{e,3}<360°$ the motion is clockwise about the earth. If $\alpha_{e,3}=180°$ the motion is directly toward the center of the earth. If $\alpha_{e,3}=0°$ or 360° the vehicle will return to the center of the earth provided the velocity at the point of exit is less than the earth-escape velocity.

With the geocentric exit conditions known, the return trajectory may now be calculated by using equations similar to those used for the earth departure trajectory (eqs. (B1) to (B11)). The eccentricity of the return trajectory is

$$\epsilon_{e,3}=\frac{1}{\cos\,(\theta_{e,3})'}\left(\frac{p_{e,3}}{r_{e,3}}-1\right) \tag{B64}$$

where

$$\frac{p_{e,3}}{r_{e,3}}=\left[\frac{V_{e,3}}{(V_{e,s})_3}\right]^2\cos^2\gamma_{e,3} \tag{B65}$$

and

$$(V_{e,s})_3=\sqrt{\frac{\mu_e}{r_{e,3}}} \tag{B66}$$

and where

$$\tan\,(\theta_{e,3})'=\tan\gamma_{e,3}\left[\frac{p_{e,3}/r_{e,3}}{(p_{e,3}/r_{e,3})-1}\right] \tag{B67}$$

The prime on $\theta_{e,3}$ denotes that $\theta_{e,3}$ is measured from the perigee radius vector of the return trajectory. This point is noted since the major axis of the return trajectory is not necessarily coincident with that of the earth departure trajectory.

The perigee radius of the return trajectory is

$$r_{e,p}=\frac{p_{e,3}}{1+\epsilon_{e,3}} \tag{B68}$$

The radius at any point during the return trajectory is

$$r_e=\frac{p_{e,3}}{1+\epsilon_{e,3}\cos\theta_e'} \tag{B69}$$

where θ_e' is measured from the perigee radius vector of the return trajectory.

The velocity at any point during the return

trajectory is

$$V_e=\sqrt{\mu_e\left(\frac{2}{r_e}-\frac{1-\epsilon_{e,3}^2}{p_{e,3}}\right)} \qquad \text{(B70)}$$

The flight-path angle at any point during the return trajectory is

$$\tan \gamma_e=\frac{\epsilon_{e,3}\sin \theta_e'}{1+\epsilon_{e,3}\cos \theta_e'} \qquad \text{(B71)}$$

Time from the point of exit from the lunar sphere of influence to any point in the return trajectory may be computed by using equations similar to (B8) to (B11). The total trip time from insertion to any point in the return trajectory is

$$t=t_3+\frac{\sin \alpha_{e,3}}{|\sin \alpha_{e,3}|}\left[t(\theta_e')-t(\theta_{e,3})'\right] \qquad \text{(B72)}$$

where $t(\theta_e')$ and $t(\theta_{e,3})'$ are the times from perigee of the return trajectory to the point in question and to the point of exit from the lunar sphere of influence, respectively. The angles and distances in equations (B57) to (B72) are shown in figures 20 and 21.

Two additional points of interest remain to be mentioned: the computation of geocentric distance and angular position with respect to the major axis of the departure trajectory during the selenocentric portion of the trajectory, and the referencing of points on the return trajectory to the departure trajectory.

The distance from the earth during the selenocentric orbit can be computed as follows:

$$r_e^2=r_m^2+D^2+2r_mD\cos\left(\theta_{m,x}-\omega_m t\right) \qquad \text{(B73)}$$

where r_m is computed from equation (B23), t is computed from equation (B34), and

$$\theta_{m,x}=\theta_m-\theta_0 \qquad \text{(B74)}$$

where θ_0 is computed from equation (B52).

The angular position of a point on the selenocentric trajectory with respect to the perigee radius vector of the departure trajectory is

$$\theta_e=\theta_{e,x}+180-\lambda \qquad \text{(B75)}$$

where

$$\theta_{e,x}=\omega_m t+\eta \qquad \text{(B76)}$$

and

$$\sin \eta=\frac{r_m}{r_e}\sin\left(\theta_{m,x}-\omega_m t\right) \qquad \text{(B77)}$$

and $\cos \eta$ is always positive.

The angular displacement of a point on the return trajectory with respect to the major axis of the departure trajectory is

$$\theta_e=\theta_e'+\Delta\lambda \qquad \text{(B78)}$$

The term $\Delta\lambda$ is defined as the angular difference between the major axes of the earth departure trajectory and return trajectory and is

$$\Delta\lambda=\theta_{e,3}-(\theta_{e,3})' \qquad \text{(B79)}$$

where $(\theta_{e,3})'$ is computed from equation (B67) and $\theta_{e,3}$ is computed from equations (B75), (B76), and (B77), with $t=t_3$. The distances and angles in equations (B73) to (B79) are shown in figures 21 and 22.

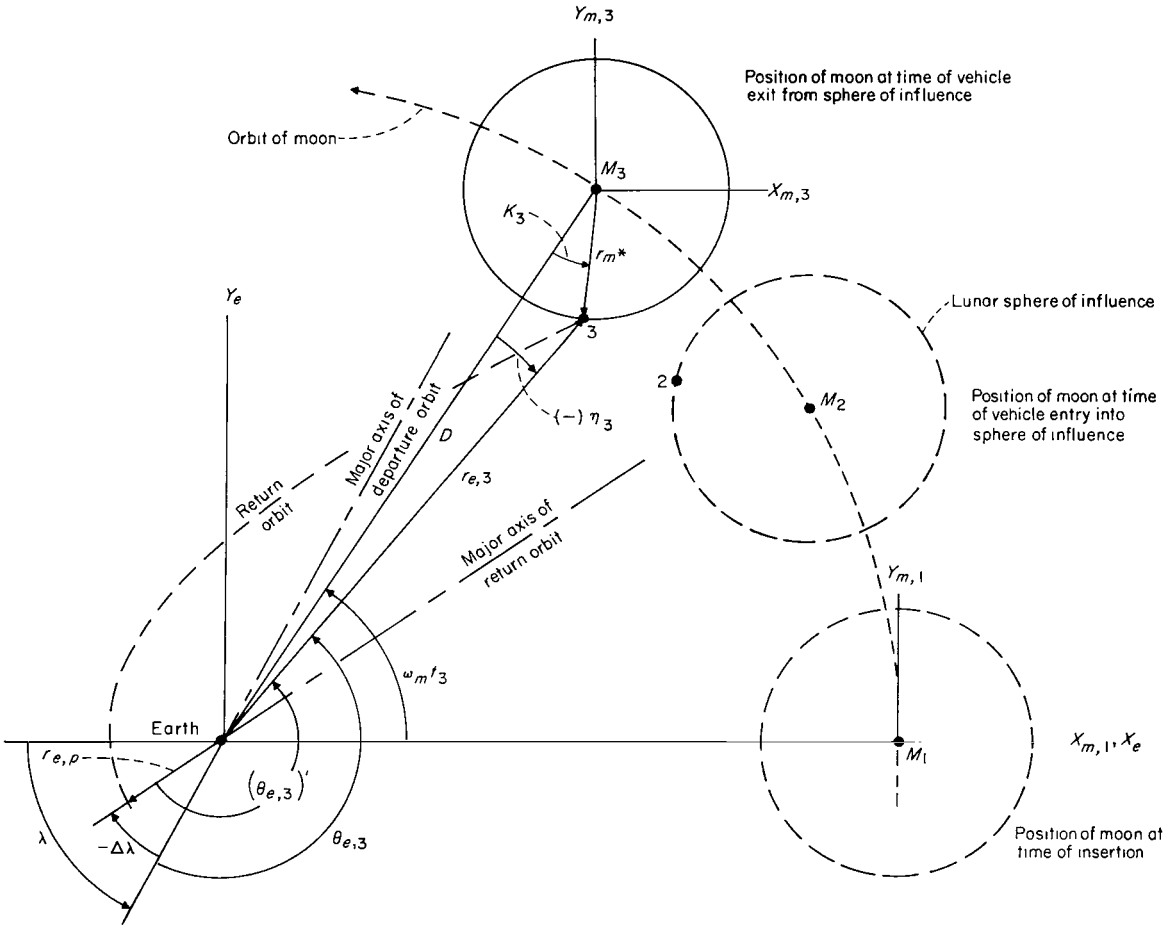

FIGURE 21.—Definition of parameters for return orbit. Positive directions shown.

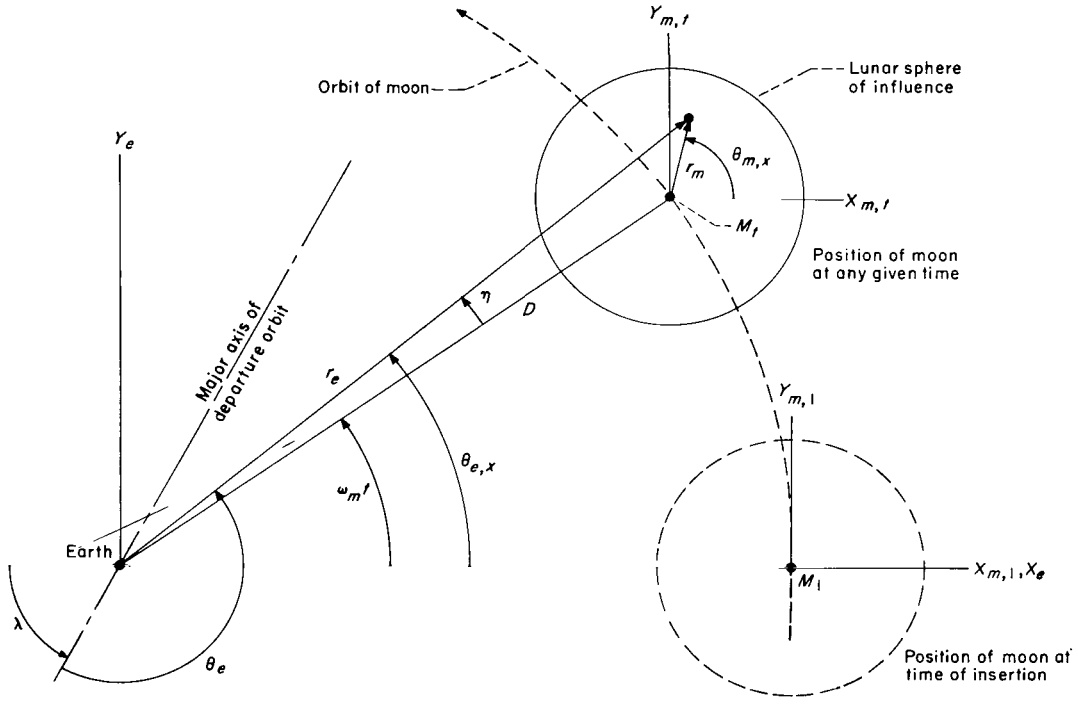

FIGURE 22.—Definition of parameters used in converting from selenocentric to geocentric coordinates. Positive directions shown.

APPENDIX C

SPHERES OF INFLUENCE OF MOON AND EARTH

SPHERE OF INFLUENCE OF MOON

For the earth-moon system, the boundary of the sphere of influence of the moon is defined as the location in space where the ratio of the force with which the earth perturbs the selenocentric motion (motion about the moon) of a vehicle to the force of the attraction of the moon on the vehicle is equal to the ratio of the force with which the moon perturbs the geocentric motion (motion about the earth) of the vehicle to the attraction of the earth on the vehicle. This definition can be written as

$$\frac{f_{P,E}}{f_{A,M}}=\frac{f_{P,M}}{f_{A,E}} \tag{C1}$$

where $f_{P,E}$ and $f_{P,M}$ represent the perturbing force of the earth and moon, respectively, and $f_{A,E}$ and $f_{A,M}$ represent the attraction of the earth and moon on the vehicle.

Pertinent relations are shown in the following sketch:

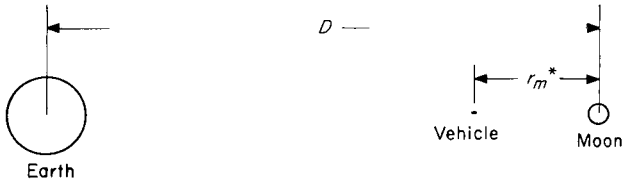

The ratio $f_{P,E}/f_{A,M}$ is determined as follows: The acceleration of the vehicle due to the moon $a_{v,M}$ is

$$a_{v,M}=\frac{Gm_m}{(r_m^*)^2} \tag{C2}$$

The acceleration of the vehicle due to the earth $a_{v,E}$ is

$$a_{v,E}=\frac{Gm_e}{(D-r_m^*)^2} \tag{C3}$$

The acceleration of the moon due to the earth $a_{m,E}$ is

$$a_{m,E}=\frac{Gm_e}{D^2} \tag{C4}$$

where G is the universal gravitational constant and m_e and m_m are the masses of the earth and moon, respectively.

The ratio $f_{P,E}/f_{A,M}$ is then

$$\frac{f_{P,E}}{f_{A,M}}=\frac{a_{v,E}-a_{m,E}}{a_{v,M}}=\frac{m_e}{m_m}(r_m^*)^3\frac{2D-r_m^*}{D^2(D-r_m^*)^2} \tag{C5}$$

In a similar manner, the ratio $f_{P,M}/f_{A,E}$ is

$$\frac{f_{P,M}}{f_{A,E}}=\frac{m_m}{m_e}(D-r_m^*)^3\frac{D+r_m^*}{D^2(r_m^*)^2} \tag{C6}$$

On substituting equations (C5) and (C6) into equation (C1), the value for the boundary of the sphere of influence of the moon is found to be

$$r_m^*=\left(\frac{D+r_m^*}{2D-r_m^*}\right)^{1/5}(D-r_m^*)\left(\frac{m_m}{m_e}\right)^{2/5} \tag{C7}$$

The perturbing effect is a maximum when the vehicle is directly between the earth and the moon and a minimum when the moon is directly between the earth and the vehicle.

Now, since $D>>r_m^*$, the radius of the sphere of influence of the moon can be given approximately by

$$r_m^*\approx\left(\frac{1}{2}\right)^{1/5}D\left(\frac{m_m}{m_e}\right)^{2/5}\approx 0.8705D\left(\frac{m_m}{m_e}\right)^{2/5} \tag{C8}$$

Taking the ratio m_m/m_e equal to 1/81.45 yields

$$r_m^*=0.1498D \tag{C9}$$

For the average circular lunar orbit, D=238,857 statute miles; therefore,

$$r_m^*=35{,}781 \text{ statute miles}$$

It is recognized that the sphere of influence as defined herein is not an exact sphere. From equation (C7) it can be shown that the sphere of influence has a radius of 32,200 statute miles for a point directly between the earth and the

moon and 39,600 miles for a point directly opposite on the other side of the moon. The value of 35,781 statute miles is about the same as the average of these two values.

SPHERE OF INFLUENCE OF EARTH

For the sun-earth system, the sphere of influence of the earth can be determined in a manner similar to the previous analysis and is

$$r_e^*=\left(\frac{H+r_e^*}{2H-r_e^*}\right)^{1/5}(H-r_e^*)\left(\frac{m_e}{m_s}\right)^{2/5} \quad \text{(C10)}$$

where H is the average distance between the earth and the sun, and m_e/m_s is the ratio of the mass of the earth to the mass of the sun.

Since $H>>r_e^*$, the radius of the sphere of influence of the earth can be given approximately by

$$r_e^*\approx 0.8705H\left(\frac{m_e}{m_s}\right)^{2/5} \quad \text{(C11)}$$

For the sun-earth system, the value for r_e^* from equation (C11) is approximately 502,000 statute miles.

REFERENCES

1. Yegorov, V. A.: Certain Problems on the Dynamics of Flight to the Moon. Rep. No. 187 (Project NY–1377), U.S. Joint Pub. Res. Service, Jan. 25, 1958, pp. 101–174.
2. Moulton, Forest Ray: An Introduction to Celestial Mechanics. Second rev. ed., The Macmillan Co., c.1914.
3. Michael, William H., Jr., and Tolson, Robert H.: Effect of Eccentricity of the Lunar Orbit, Oblateness of the Earth, and Solar Gravitational Field on Lunar Trajectories. NASA TN D–227, 1960.
4. Lieske, H. A.: Circumlunar Trajectory Studies. [Paper] P–1441, The RAND Corp., June 25, 1958.
5. Michael, William H., Jr., and Tolson, Robert H.: Three-Dimensional Lunar Mission Studies. NASA MEMO 6-29-59L, 1959.
6. Michael, William H., Jr., and Crenshaw, Jack W.: Trajectory Considerations for Circumlunar Missions. Paper No. 61–35, Inst. Aerospace Sci., Jan. 1961.
7. Weber, Richard J., Pauson, Werner M., and Burley, Richard R.: Lunar Trajectories. NASA TN D–866, 1961.

U.S. GOVERNMENT PRINTING OFFICE:1963